Fraunhofer Institut
Techno- und
Wirtschaftsmathematik

A. Wiegmann

Computation of the permeability of porous materials from their microstructure by FFF-Stokes

Berichte des Fraunhofer ITWM, Nr. 129 (2007)

ISSN 1434-9973

Bericht 129 (2007)

Die Veröffentlichungen in der Berichtsreihe des Fraunhofer ITWM können bezogen werden über:

Fraunhofer-Institut für Techno- und
Wirtschaftsmathematik ITWM
Fraunhofer-Platz 1

67663 Kaiserslautern
Germany

Telefon: +49(0)631/3160 0-0
Telefax: +49(0)631/3160 0-1099
E-Mail: info@itwm.fraunhofer.de
Internet: www.itwm.fraunhofer.de

Vorwort

Das Tätigkeitsfeld des Fraunhofer-Instituts für Techno- und Wirtschaftsmathematik ITWM umfasst anwendungsnahe Grundlagenforschung, angewandte Forschung sowie Beratung und kundenspezifische Lösungen auf allen Gebieten, die für Techno- und Wirtschaftsmathematik bedeutsam sind.

In der Reihe »Berichte des Fraunhofer ITWM« soll die Arbeit des Instituts kontinuierlich einer interessierten Öffentlichkeit in Industrie, Wirtschaft und Wissenschaft vorgestellt werden. Durch die enge Verzahnung mit dem Fachbereich Mathematik der Universität Kaiserslautern sowie durch zahlreiche Kooperationen mit internationalen Institutionen und Hochschulen in den Bereichen Ausbildung und Forschung ist ein großes Potenzial für Forschungsberichte vorhanden. In die Berichtreihe sollen sowohl hervorragende Diplom- und Projektarbeiten und Dissertationen als auch Forschungsberichte der Institutsmitarbeiter und Institutsgäste zu aktuellen Fragen der Techno- und Wirtschaftsmathematik aufgenommen werden.

Darüber hinaus bietet die Reihe ein Forum für die Berichterstattung über die zahlreichen Kooperationsprojekte des Instituts mit Partnern aus Industrie und Wirtschaft.

Berichterstattung heißt hier Dokumentation des Transfers aktueller Ergebnisse aus mathematischer Forschungs- und Entwicklungsarbeit in industrielle Anwendungen und Softwareprodukte – und umgekehrt, denn Probleme der Praxis generieren neue interessante mathematische Fragestellungen.

Prof. Dr. Dieter Prätzel-Wolters
Institutsleiter

Kaiserslautern, im Juni 2001

COMPUTATION OF THE PERMEABILITY OF POROUS MATERIALS FROM THEIR MICROSTRUCTURE BY FFF-STOKES

A. WIEGMANN

Abstract. A fully automatic procedure is proposed to rapidly compute the permeability of porous materials from their binarized microstructure. The discretization is a simplified version of Peskin's Immersed Boundary Method, where the forces are applied at the no-slip grid points.

As needed for the computation of permeability, steady flows at zero Reynolds number are considered. Short run-times are achieved by eliminating the pressure and velocity variables using an Fast Fourier Transform-based and 4 Poisson problem-based fast inversion approach on rectangular parallelepipeds with periodic boundary conditions. In reference to calling it a fast method using fictitious or artificial forces, the implementation is called *FFF-Stokes*.

Large scale computations on 3d images are quickly and automatically performed to estimate the permeability of some sample materials. A matlab implementation is provided to allow readers to experience the automation and speed of the method for realistic three-dimensional models.

Date: November 14, 2007.

E-mail: `wiegmann@itwm.fraunhofer.de`. The author is grateful for financial support by the Kaiserslautern Excellence Cluster Dependable Adaptive Systems and Mathematical Modelling.

1. Introduction

Recent technological advances allow the reconstruction of realistic three-dimensional images of many porous materials [24, 8]. There is great interest in performing flow simulations in order to relate the obtained three-dimensional micro structures with the macroscopically measureable permeability of these materials [25, 18, 21, 10]. The book [26] gives a good introduction and overview to this topic.

The goal of this work is to develop a method that can perform such computations as quickly as possible, and with as little preprocessing as possible. When this is achieved, the method can also be used in a design cycle, where virtual sructures are generated and evaluated with respect to their permeability.

To compute the permeability of a material, first the stationary Stokes equations are solved and then the velocities are averaged. There are two fundamental challenges.

First, the rapid and reliable generation of computational grids for very complex geometries.

Second, the efficient solution of very large linear systems of equations.

The first task is solved by simply taking the image itself as the grid. All that is needed is a binarization of the image, where the two states empty and solid are marked. The pore space is then given by the collection of empty cells, and the obstacles are defined by the solid cells. The resulting cubic grid cells are commonly referred to as *voxels*.

Such grids are used very successfully in the lattice Boltzmann method [3] for the computation of material permeabilities. The success rate of grid generation is 100%, the run-times of the automatic grid generator are negligable compared to the solver. In the staggered grid approach, the velocities are defined on their respective voxel-faces and the pressure variables are defined in the center of the voxel. From [22] the permeability tensor can be computed by solving three Stokes problems with periodic boundary conditions and a uniform body force in the pores that is aligned with one of the three coordinate directions.

The second task is tackled by using a grid-aligned version of Peskin's immersed boundary method [16]. Artificial forces allowing to extend the Stokes equations to the whole domain was used by many different groups [6, 4, 11, 28]. But differently from those works, here there is no immersed boundary. The forces are simply introduced at the grid points where the no-slip conditions should be enforced. This simplification is possible because only Stokes-flows are considered, and this simplification does not cause additional loss of accuracy because the obstacles are only given with the resolution of a voxel.

Most similar to our use of artificial forces is the work by Jung and Torquato [10] because they also implement boundary conditions through forces to evaluate permeabilities. But instead of their Crank-Nicholson method driving a time-dependent problem to steady-state, we directly discretize and solve the steady-state.

The newly introduced forces on the surfaces of the solids and velocities and pressure variables inside the solids are viewed as additional unknowns. The new velocity and pressure variables are accounted for by the extension of the conservation of momentum and conservation of mass into the solids. In the interior of the solids, the forces are zero. Together with the no-slip conditions this means the velocity is zero inside the

obstacles, and the pressure is constant. The new force variables are defined by the no-slip conditions on the forces.

In a Schur-complement formulation, one is only left with the discretization of the no-slip boundary conditions on the solid walls where the variables are the auxiliary forces on the solid walls. The meaning of the Schur-complement is to embed the forces as singular forcing terms in the volume, then to solve a forced Stokes problem on the volume without obstacles and with periodic boundary conditions and lastly, to reduce the solution of this Stokes problem to the surfaces of the obstacles.

This follows in spirit the long traditions of fictitious domain methods ([13] and references therein) and capacitance matrix methods ([17]). See also [2] and references therein. [9] has extracted the general case where such fast methods apply: when complete rows of the system matrix agree with the preconditioner, the iterations can be reduced to a sparse subspace.

The discretization applies on a staggered grid (see §3.1 for details), takes advantage of many well known matrix properties of finite difference matrices (see §3.3) and the equally well-known fast Poisson solvers for rectangular domains with periodic boundary conditions ([23, 5]). In summary, three steps are required.

(1) In §2, the well known solution of the **Stokes equations by four Poisson equations** is carried over to the **discrete case in the presence of no-slip conditions** on the surface of the fibers.
(2) Then a **symmetric** Schur-complement formulation is derived that makes use of fast Poisson solvers **on periodic domains**.
(3) The Null-space of the discretized Laplacian for periodic boundary conditions is judiciously taken care of in a **singular Schur-complement formulation**.

The discretization (§3) results in a symmetric Schur-complement (§4) for the auxiliary forces on the fiber surfaces which can be solved very efficiently with an appropriate choice of conjugate gradiens, namely `MINRES`.

The examples section §5 illustrates the first order convergence and efficiency of the approach for computing permeabilities of several sample materials.

[30] lists a `Matlab` implementation to allow readers to experience both the automation and speed of the method for realistic three-dimensional models.

2. Equations

2.1. **The Steady Stokes Equation.** We use the following notation for the incompressible steady Stokes equation and the boundary conditions for the computation of the permability tensor of porous materials.

$$\begin{aligned} -\mu\Delta\mathbf{u} + \nabla p &= \mathbf{f} \text{ in } \Omega \setminus G, && (1)\\ \operatorname{div} \mathbf{u} &= 0 \text{ in } \Omega \setminus G, && (2)\\ \mathbf{u}(x + il_x, y + jl_y, z + kl_z) &= \mathbf{u}(x, y, z) \text{ for } i, j, k \in \mathbf{Z}, && (3)\\ p(x + il_x, y + jl_y, z + kl_z) &= p(x, y, z) \text{ for } i, j, k \in \mathbf{Z}, \\ \mathbf{u} &= 0 \text{ on } \partial G. && (4) \end{aligned}$$

(1), (2) and (3) are the conservation of momentum, conservation of mass and periodicity of the velocities and pressure, respectively. G with surface ∂G is the volume that is occupied by solid material and $\Omega = [0, l_x] \times [0, l_y] \times [0, l_z]$ is the computational box **including** the volume occupied by both solid and void. $\mathbf{u}$ is the velocity vector with components u, v and w, $\mathbf{f}$ is the density of a body force in the pore portion of the computational box with components f_x, f_y and f_z, and p is the pressure. By div we mean the application of the divergence operator $(\partial_x, \partial_y, \partial_z)$ and (4) is the no-slip boundary condition on the surfaces of the solid.

2.2. **Stokes via Four Poisson Problems.** For sufficiently regular $\mathbf{f}$, $\mathbf{u}$ and p, the steady Stokes equations decouple into four Poisson problems [12] by taking advantage of the fact that the Laplace and divergence operators commute. Applying the divergence to the momentum equations and using the conservation of mass yields

$$\text{div } \nabla p = \Delta p = \text{ div } (\mu \Delta \mathbf{u}) + \text{ div } \mathbf{f} = \mu \Delta (\text{ div } \mathbf{u}) + \text{ div } \mathbf{f} = \text{ div } \mathbf{f}.$$

Hence, the Stokes problem could be solved as four Poisson problems

$$\begin{aligned} \Delta p &= \text{ div } \mathbf{f} \text{ in } \Omega \setminus G, \\ \mu \Delta u &= \frac{\partial p}{\partial x} - f_x \text{ in } \Omega \setminus G, \\ \mu \Delta v &= \frac{\partial p}{\partial y} - f_y \text{ in } \Omega \setminus G, \\ \mu \Delta w &= \frac{\partial p}{\partial z} - f_z \text{ in } \Omega \setminus G, \\ \mathbf{u} &= 0 \text{ on } \partial G, \end{aligned}$$

if only we knew what boundary conditions to use for the pressure. Later it turns out that implicitly and discretely, we do know them!

Equation (17) suggests that the pressure on the boundary should be given by the the sum of two terms, one being $-\frac{\partial}{\partial \mathbf{n}} (\mathbf{u} \cdot \mathbf{n})$ and the other term only depending on the integral of the body force, appropriately distributed to the boundaries, and dottet with the normal direction $\mathbf{n}$ which points from $\Omega \setminus G$ into G.

2.3. **Calculation of the permeability.** According to Darcy's law, the through permeability κ_{zz} in $[m^2]$ is defined for a porous material aligned with the $x-$ and $y-$ coordinates as

$$\kappa_{zz} = \mu \frac{d}{\Delta P} \frac{Q}{A}.$$

Here μ is the fluid viscosity in $[kg/(ms)]$, d is the thickness of the probe in $[m]$, ΔP is the applied pressure difference in $[kg/(ms^2)]$, Q is the mass flux in $[m^3/s]$ and A is the cross section area in $[m^2]$.

Noting that $\frac{Q}{A}$ is the mean velocity $\bar{w}$ and rearranging slightly, we get

$$\bar{w} = \frac{\kappa_{zz}}{\mu} \frac{\Delta P}{d}. \tag{5}$$

What is the meaning of ΔP in our above setting (1)—(4), i.e. for periodic boundary conditions? The pressure variable p agrees on opposite sides, so its contribution to

ΔP valishes. However, we may think of the body force as the gradient of the applied pressure difference, $\nabla \tilde{p} = -\mathbf{f}$.

Periodic boundary conditions usually lead to non-zero mean velocity components also in the two directions that lie perpendicular to the applied pressure difference. This allows the computation of the full permeability tensor, which generalizes Darcy's original "through-permeability" κ_{zz}. Now κ denotes the tensor of permeabilities and $\bar{\mathbf{u}} = (\bar{u}, \bar{v}, \bar{w})$ the vector of mean velocities. Three Boundary Value Problems should be considered to completely determine κ. The calculations become particularly simple for pressure drops proportional to the length of the domain. $\Delta P = l_x$ for the $x-$direction results in $\nabla \tilde{p} = -\mathbf{f_1} = -(1,0,0)'$, $\Delta P = l_y$ for the $y-$direction results in $\nabla \tilde{p} = -\mathbf{f_2} = -(0,1,0)'$ and $\Delta P = l_z$ for the $z-$direction results in $\nabla \tilde{p} = -\mathbf{f_3} = -(0,0,1)'$, respectively. The resulting vectors of mean velocities are $\bar{\mathbf{u}}_\mathbf{1}$, $\bar{\mathbf{u}}_\mathbf{2}$ and $\bar{\mathbf{u}}_\mathbf{3}$, respectively.

Recalling that the pressure gradient points from the larger pressure in front to the lower pressure behind the probe, (5) becomes

$$\bar{\mathbf{u}} = -\frac{\kappa}{\mu} \nabla \tilde{p}. \tag{6}$$

The choice of forces in the Cartesian directions allows the computation of the permeability tensor one column at the time:

$$\begin{pmatrix} \kappa_{xx} \\ \kappa_{yx} \\ \kappa_{zx} \end{pmatrix} = \mu \begin{pmatrix} \bar{u}_1 \\ \bar{v}_1 \\ \bar{w}_1 \end{pmatrix}, \begin{pmatrix} \kappa_{xy} \\ \kappa_{yy} \\ \kappa_{zy} \end{pmatrix} = \mu \begin{pmatrix} \bar{u}_2 \\ \bar{v}_2 \\ \bar{w}_2 \end{pmatrix}, \begin{pmatrix} \kappa_{xz} \\ \kappa_{yz} \\ \kappa_{zz} \end{pmatrix} = \mu \begin{pmatrix} \bar{u}_3 \\ \bar{v}_3 \\ \bar{w}_3 \end{pmatrix}.$$

As the material permeability is independent of the viscosity, the viscosity may be chosen as 1. In this case, the column of the permeability tensor is simply the mean velocity resulting from the unit force applied in the corresponding direction. This is illustrated in the accompanying matlab program [30].

3. Discretization

3.1. **The staggered grid. u** and p are discretized on a staggered grid derived from a uniform Cartesian grid with mesh size h. We will sometimes refer to the U-grid, V-grid, W-grid and P-grid and let

$$n = n_x n_y n_z$$

denote the number of voxel centers.

Cell centers are located at $\{0.5h, 1.5h, ..., (n_x - 0.5)h\} \times \{0.5h, 1.5h, ..., (n_y - 0.5)h\} \times \{0.5h, 1.5h, ..., (n_z - 0.5)h\}$, and the variables have the following meaning: for $i = 1, 2, \ldots, n_x$, $j = 1, 2, \ldots, n_y$ and $k = 1, 2, \ldots, n_z$:

$P_{i,j,k}$	is pressure at	$((i-0.5)h, (j-0.5)h, (k-0.5)h)$,
$U_{i,j,k}$	is x-component of velocity at	$((i-1.0)h, (j-0.5)h, (k-0.5)h)$,
$V_{i,j,k}$	is y-component of velocity at	$((i-0.5)h, (j-1.0)h, (k-0.5)h)$,
$W_{i,j,k}$	is z-component of velocity at	$((i-0.5)h, (j-0.5)h, (k-1.0)h)$.

Figure 1 illustrates the staggered grid and the meaning of the variables.

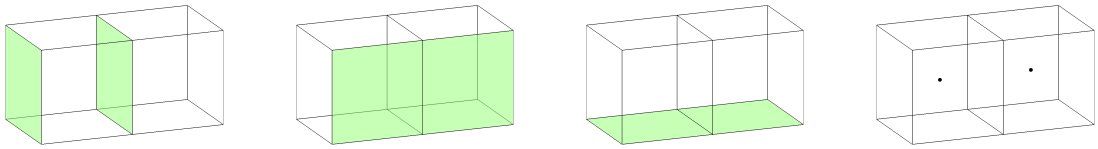

FIGURE 1. *a) The discrete velocity variable in the x-direction approximates the continuous velocity at the center of the left voxel face. b) The discrete velocity variable in the y-direction approximates the continuous velocity at the center of the front voxel face. c) The velocity variable in the z-direction approximates the continuous velocity variable at the center of the bottom voxel face. d) The discrete pressure variable approximates the continuous pressure at the voxel center.*

Definition 3.1. *Solid surface faces on a MAC grid are faces of solid voxels so that one of the 6 neighboring faces on the same grid lies in the flow domain. See* `find_surface` *routine in* [30].

By periodicity, P_{i,j,n_x} is a neighbor of $P_{i,j,1}$, etc. There are three different sets of indices for the surface variables indexed $1, 2, \ldots, m_x$, $1, 2, \ldots, m_y$ and $1, 2, \ldots, m_z$ on the U-, V- and W-grids, respectively. The discrete no-slip boundary condition must be imposed at the locations of these surface variables which are marked by filled symbols in Figure 2. This figure also illustrates the reason why the method converges only with first order even when the true geometry is represented exaclty by the voxels: the no-slip condition in the tangential direction is enforced half a mesh width away from the true voxel surface. This leads to slightly higher velocities than the correct boundary location would yield.

Remark 3.1. *On the staggered grid, no boundary conditions are needed for p. ∇p is evaluated only on voxel faces inside the flow domain, where both neighboring values of p are "interior values".*

3.2. **Review of discrete operators and their properties.** Using the index map

$$l = i + n_x((j-1) + n_y(k-1)),$$

geometry-dependent embedding operators for the three types of surface variables may be defined:

$E_x \in \mathbf{R}^{n \times m_x}$	maps the U-surface variables to their 3d location,
$E_y \in \mathbf{R}^{n \times m_y}$	maps the V-surface variables to their 3d location and
$E_z \in \mathbf{R}^{n \times m_z}$	maps the W-surface variables to their 3d location.

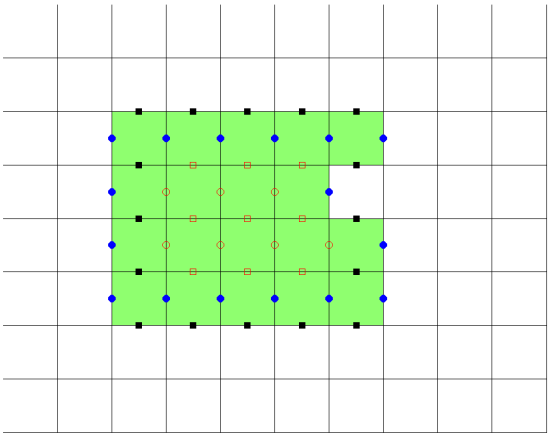

FIGURE 2. *The auxiliary variables in the horizontal (circles) and vertical directions (squares). Empty symbols denote positions where the auxiliary forces can be set to zero and the variables are not surface variables because their 4 grid neighbors are all interior to the green domain. In 3d the 6 grid neighbors have to be considered.*

To extend operators and variables to Ω, we need more notation:

$$\begin{aligned} \Sigma_l &= (1,1,\ldots,1)' \in \mathbf{R}^l \\ O_l &= (0,0,\ldots,0)' \in \mathbf{R}^l \\ S^l &= \mathbf{R}^l \setminus \{\Sigma_l\} \\ M_l &= \frac{1}{l}\Sigma_l\Sigma_l' \in \mathbf{R}^{l\times l} \\ P_l &= (I_l - M_l) \end{aligned}$$

The inner product of a vector with Σ_l is the sum of that vector. S^l is the l-dimensional space of vectors in $\mathbf{R}^l$ with sum zero. M_l applied to a vector yields a constant vector with the same average value. I_l is the $l-$dimensional identity and P_l is the orthogonal projector from $\mathbf{R}^l \to S^l$.

Furthermore, we will use

$$\begin{aligned} \Psi_x &= E_x P_{m_x} \in \mathbf{R}^{n\times m_x}, \\ \Psi_y &= E_y P_{m_y} \in \mathbf{R}^{n\times m_y}, \\ \Psi_z &= E_z P_{m_z} \in \mathbf{R}^{n\times m_z}. \end{aligned}$$

Ψ_x embeds the projection from $\mathbf{R}^{m_x} \to S^{m_x}$ in $\mathbf{R}^n$. Ψ_y and Ψ_z repsectively embed the projection from $\mathbf{R}^{m_y} \to S^{m_y}$ in $\mathbf{R}^n$ and the projection from $\mathbf{R}^{m_z} \to S^{m_z}$ in $\mathbf{R}^n$.

3.3. **Properties of finite difference matrices.** The standard difference operators have several well known important properties which we summarize here for completeness and later reference. The notation follows [7].

Definition 3.2. *The matrix $D^+(n)$ with entries*

$$D^+(n)_{i,j} = \delta_{i,j+1} - \delta_{i,j}, \text{ where } i,j \in \{1,2,\ldots,n\}$$

is the periodic 1d unit forward difference matrix *for n cells. By periodicity $j = 0$ is identified with $j = n$ and $\delta_{i,j}$ is the Kronecker delta that is equal to 1 if $i = j$ and equal to 0 otherwise. Similarly, the matrix $D^-(n)$ with entries*

$$D^-(n)_{i,j} = \delta_{i,j} - \delta_{i,j-1}, \text{ where } i,j \in \{1,2,\ldots,n\}$$

is the periodic 1d unit backward difference matrix *for n cells. Periodic differences on the uniform grid with mesh width h can be derived from the unit differences through division by h.*

Definition 3.3. *The matrix*

$$\Delta(n) = D^+(n)D^-(n)$$

is the periodic 1d unit Laplace matrix *for n cells. The periodic Laplace matrix on the uniform grid with mesh width h can be derived from the unit matrix through division by h^2.*

Definition 3.4. *The centered 2- and 3-dimensional difference matrices can be derived as follows:*

$$\begin{aligned}
D^c_x(n_x) &= (2h)^{-1}\left(D^+(n_x) + D^-(n_x)\right)\\
D_{xx}(n_x) &= h^{-2}D^+(n_x)D^-(n_x)\\
D_{zz}(n_x,n_y,n_z) &= h^{-2}I(n_x)\otimes I(n_y)\otimes \Delta(n_z)\\
D_{yy}(n_x,n_y,n_z) &= h^{-2}I(n_x)\otimes \Delta(n_y)\otimes I(n_z)\\
D_{xx}(n_x,n_y,n_z) &= h^{-2}\Delta(n_x)\otimes I(n_y)\otimes I(n_z)
\end{aligned}$$

where the tensor product notation $\otimes$ means that the matrix on the left is a block that gets multiplied with the entries of the matrix on the right, and $I(n)$ is the $n-$dimensional identity matrix.

Remark 3.2. *The centered difference operators approximate the first and second derivatives of a periodic function at a grid point. The forward difference approximates the first derivative of a periodic function at the center between a grid point and its successor (with the correct periodic interpretation). The backward difference approximates the first derivative of a periodic function at the center between a grid point and its predecessor (with the correct periodic interpretation). With this interpretation regarding the location, all approximations are second order. This makes the staggered grid approach second order accurate for interior empty cells.*

Proposition 3.5. *The periodic difference operators in 1, 2 and 3 dimensions have the following properties: for $n_x, n_y, n_z \in \mathbb{N}$, $s,t \in \{+,-\}$ and $a,b \in \{x,y,z\}$:*

(1) *The forward and backward operators are negative conjugates:*

$$D^+_a(n_x,n_y,n_z) = D^-_a(n_x,n_y,n_z)'.$$

(2) *The forward and backward operators commute:*

$$D_a^s(n_x,n_y,n_z)D_b^t(n_x,n_y,n_z) = D_b^t(n_x,n_y,n_z)D_a^s(n_x,n_y,n_z).$$

Proof. The proof is purely algebraic and can be found, for example, in [27]. □

Proposition 3.6. *For all* $\mathbf{v} \in \mathbf{R^n}$, *for all* $a \in \{x,y,z\}$, *and for all* $s \in \{+,-\}$, $D_a^s(n_x,n_y,n_z)\mathbf{v} \in \mathbf{S^n}$.

Proof. Because every entry in $\mathbf{v}$ appears once with the positive and once with the negative sign, this property is obvious for *periodic* difference operators. □

With the understanding that all matrices are intended for three-dimensional voxel geometries of lengths n_x, n_y and n_z, respectively, where the lengths are positive integers we drop the arguments (n_x,n_y,n_z) from all subsequent difference matrices. Length 1 is allowed, the matrix "shrinks" to a lower dimensional operator.

Proposition 3.7. *The seven point stencil discretization of the discrete Laplacian in 3d is*

$$\begin{aligned}\Delta_h &= -\left(D_x^+D_x^- + D_y^+D_y^- + D_z^+D_z^-\right)\\ &= -\left(D_x^-D_x^+ + D_y^-D_y^+ + D_z^-D_z^+\right)\end{aligned}$$

Proof. The proof is purely algebraic and can be found in [27]. □

Proposition 3.8. *The restriction of* Δ_h *to* S^n *is an invertible operator on* S^n.

Proof. We denote the 3-dimensional discrete Fourier Transform (DFT) of $\mathbf{U}$ by $\mathcal{F}\mathbf{U}$. For $(l,m,p) \neq (1,1,1)$, where the indices in Fourier space l,m and p run from 1 to n_x,n_y and n_z, respectively, one finds (see [29]) that

$$\Delta_h\mathbf{U} = \mathbf{F}$$

implies

$$(\mathcal{F}\mathbf{U})_{l,m,p} = \frac{h^2\left(\mathcal{F}\mathbf{F}\right)_{l,m,p}}{\left\{2\cos\left(\frac{2(k-1)\pi}{n_x}\right) + 2\cos\left(\frac{2(m-1)\pi}{n_y}\right) + 2\cos\left(\frac{2(p-1)\pi}{n_z}\right) - 6\right\}}.$$

Since $\mathbf{F} \in S^n$ means

$$\left(\mathcal{F}\mathbf{F}\right)_{1,1,1} = 0 \tag{7}$$

we can simply map $(\mathcal{F}\mathbf{U})_{1,1,1}$ to zero to define the inverse $\Delta_h^\dagger$ of Δ_h on S^n as follows: For $\mathbf{F} \in S^n$,

$$\mathbf{U} = \Delta_h^\dagger\mathbf{F} = h^2\mathcal{F}^{-1}\left(\mathcal{D}\mathcal{F}\mathbf{F}\right)$$

where $\mathcal{F}^{-1}$ means application of the inverse discrete Fourier transform and $\mathcal{D}$ is a diagonal matrix with $l = i + n_x((j-1) + n_y(k-1))$ and entries

$$D_{ll} = \begin{cases} 0, & l = 1 \\ \left(2\cos\left(\frac{2(k-1)\pi}{n_x}\right) + 2\cos\left(\frac{2(m-1)\pi}{n_y}\right) + 2\cos\left(\frac{2(p-1)\pi}{n_z}\right) - 6\right)^{-1}, & l = 2,3,\ldots n \end{cases}.$$

□

Remark 3.3. *The method of solving partial differential equations by FFT used in the proof of Proposition 3.8 is known since the 1960's. An overview can be found in* [23]. *For the sake of simplicity, our implementation (see* [30]*) follows* [29] *in that we actually perform three-dimensional Fourier-transforms. Solving a tri-diagonal system* [23] *in the third direction would be even more efficient.*

3.4. **The embedded discretized Stokes problem.** The Stokes equations are discretized on a staggered grid by applying specifically chosen matching discrete operators for the gradient (backward differences) and divergence (forward differences) operators:

$$\begin{aligned} -\mu\ \tilde{\Delta}_h\ \tilde{\mathbf{U}} + D_x^- \tilde{\mathbf{P}} &= \tilde{\mathbf{F}}_x \text{ in } \Omega \setminus G, \\ -\mu\ \tilde{\Delta}_h\ \tilde{\mathbf{V}} + D_y^- \tilde{\mathbf{P}} &= \tilde{\mathbf{F}}_y \text{ in } \Omega \setminus G, \qquad (8) \\ -\mu\ \tilde{\Delta}_h\ \tilde{\mathbf{W}} + D_z^- \tilde{\mathbf{P}} &= \tilde{\mathbf{F}}_z \text{ in } \Omega \setminus G, \\ \tilde{D}_x^+ \tilde{\mathbf{U}} + \tilde{D}_y^+ \tilde{\mathbf{V}} + \tilde{D}_z^+ \tilde{\mathbf{W}} &= \mathbf{O}_n \text{ in } \Omega \setminus G, \qquad (9) \\ \tilde{\mathbf{U}} &= \mathbf{O}_{m_x} \text{ on } \partial G, \\ \tilde{\mathbf{V}} &= \mathbf{O}_{m_y} \text{ on } \partial G, \qquad (10) \\ \tilde{\mathbf{W}} &= \mathbf{O}_{m_z} \text{ on } \partial G. \end{aligned}$$

By the tilde on the operators and variables we indicate that they are only valid on those portions of the grid that lie in the pores $\Omega \setminus G$. We repeat that on the staggered grid one needs no boundary conditions for the pressure since the forward differences in U, V and W each live on the P- grid, and the backward differences in P live on the U-, V- and W- grids. The backward differences are only applied across cell boundaries in the interior of the flow domain. Similarly, the forward differences in (9) are evaluated only across cell centers inside the flow domain, using the boundary conditions (10).

The Stokes equations can be rescaled with respect to viscosity and extended to the rectangular parallelepiped:

$$\begin{aligned} -\Delta_h\ \bar{\mathbf{U}} + D_x^- \bar{\mathbf{P}} - \Psi_x \mathbf{F}_x &= \bar{\mathbf{F}}_x, \\ -\Delta_h\ \bar{\mathbf{V}} + D_y^- \bar{\mathbf{P}} - \Psi_y \mathbf{F}_y &= \bar{\mathbf{F}}_y, \qquad (11) \\ -\Delta_h\ \bar{\mathbf{W}} + D_z^- \bar{\mathbf{P}} - \Psi_z \mathbf{F}_z &= \bar{\mathbf{F}}_z, \\ D_x^+ \bar{\mathbf{U}} + D_y^+ \bar{\mathbf{V}} + D_z^+ \bar{\mathbf{W}} &= \mathbf{O}_n, \qquad (12) \\ E_x' \bar{\mathbf{U}} &= \mathbf{O}_{m_x}, \\ E_y' \bar{\mathbf{V}} &= \mathbf{O}_{m_y}, \qquad (13) \\ E_z' \bar{\mathbf{W}} &= \mathbf{O}_{m_z}. \end{aligned}$$

$\bar{\mathbf{F}}_x$, $\bar{\mathbf{F}}_y$ and $\bar{\mathbf{F}}_z$ are vectors that are defined on the original domain, on the boundaryies of the obstacles and inside the obstacles. They agree with the given forces except for a division by the viscosity $\tilde{\mathbf{F}}_x/\mu$, $\tilde{\mathbf{F}}_y/\mu$ and $\tilde{\mathbf{F}}_z/\mu$, respectively, on $\Omega \setminus G$. They are zero inside the obstacles G and are chosen constant on the boundaries of the obstacles ∂G, $\bar{\mathbf{F}}_x|_{\partial G} \equiv -\left(\sum \tilde{\mathbf{F}}_x/\mu\right)/m_x$, $\bar{\mathbf{F}}_y|_{\partial G} \equiv -\left(\sum \tilde{\mathbf{F}}_y/\mu\right)/m_y$ and $\bar{\mathbf{F}}_z|_{\partial G} \equiv -\left(\sum \tilde{\mathbf{F}}_z/\mu\right)/m_z$. This means they sum to zero on Ω, i.e. $\bar{\mathbf{F}}_x \in S^n$, $\bar{\mathbf{F}}_y \in S^n$

and $\bar{\mathbf{F}}_z \in S^n$. Similarly, $\bar{\mathbf{U}}$, $\bar{\mathbf{V}}$ and $\bar{\mathbf{W}}$ are vectors that agree with $\tilde{\mathbf{U}}$, $\tilde{\mathbf{V}}$ and $\tilde{\mathbf{W}}$ on $\Omega \setminus G$ and vanish on the boundary δG and inside G. $\bar{\mathbf{P}}$ is the rescaled pressure vector that agrees with the original pressure divided by viscosity $\bar{\mathbf{P}} = \tilde{P}/\mu$ on $\Omega \setminus G$ and vanishes on the rest of Ω.

$\mathbf{F}_x$, $\mathbf{F}_y$ and $\mathbf{F}_z$ are vectors of fictitious forces on ∂G. Note that these forces can be computed from the extended velocities and pressure. They can be proven to each sum to zero by the choice of $\bar{\mathbf{F}}_x$, $\bar{\mathbf{F}}_y$ and $\bar{\mathbf{F}}_z$ and the fact that the discrete Laplace operator and each component of the discrete gradient operator map $\mathbf{R}^n$ to S^n. Thus, $\Psi_x \mathbf{F}_x = E_x \mathbf{F}_x$, $\Psi_y \mathbf{F}_y = E_y \mathbf{F}_y$ and $\Psi_z \mathbf{F}_z = E_z \mathbf{F}_z$.

Theorem 3.9. *There exists a solution of (11)-(13).*

Proof. Sketch: By standard arguments, there exists a unique solution of the original problem in the pores, (8) – (10). The complement of the pores, the interior of G, may consist of one or several compact components. In G, the trivial solution of zero velocities and zero pressure solves the boundary value problem(s) with zero velocities (no-slip) on the boundaries. Combining the solutions in the pores, on the obstacle surface and inside the obstacles results in velocities and pressure on Ω that satisfy the Stokes equations with given forces in the pores and zero forces inside the obstacles. The values of the velocities and pressures on and neighboring the surfaces determine force values on the surfaces, and thus a solution is constructed.

□

Remark 3.4. *The solution is by no means unique; the trivial extension by zero pressure is not the only extension into G. Numerical experiments for small examples suggest the following estimate for dimension the of the null-space $\mathcal{N}$ of (11)-(13):*

$$dim\ \mathcal{N} \approx 7 + max(\#S\ -\ \#F\ ,1),$$

where $\#S$ is the number of solid voxels and $\#F$ is the number of interior faces inside the solid voxels. In Figure 2, $\#S$ is the number of green squares while $\#F$ is the number of empty symbols.

To achieve symmetry of the final Schur-complement we note that P_l is symmetric and $P_l O_l = O_l$. We keep (11) and (12) for our auxiliary solution $\mathbf{U}$, $\mathbf{V}$ and $\mathbf{W}$ but replace (13) by

$$\begin{aligned} \Psi_x' \mathbf{U} &= \mathbf{O}_{m_x}, \\ \Psi_y' \mathbf{V} &= \mathbf{O}_{m_y}, \\ \Psi_z' \mathbf{W} &= \mathbf{O}_{m_z}. \end{aligned} \tag{14}$$

Remark 3.5. *For future reference, we consider the general case of arbitrary Dirichlet boundary conditions which includes no-slip boundary conditions.*

$$\begin{aligned} \Psi_x' \mathbf{U} &= P_{m_x} \mathbf{U}_0, \\ \Psi_y' \mathbf{V} &= P_{m_y} \mathbf{V}_0, \\ \Psi_z' \mathbf{W} &= P_{m_z} \mathbf{W}_0. \end{aligned} \tag{15}$$

In this case, the extension of the velocities into G is not zero but satisfies the boundary conditions "as solution inside the solid".

We can look at the modified equations because we can always find the solution of the original problem $\bar{\mathbf{U}}$, $\bar{\mathbf{V}}$, $\bar{\mathbf{W}}$ and $\bar{\mathbf{P}}$ from the solution of the new problem $\mathbf{U}$, $\mathbf{V}$, $\mathbf{W}$ and $\mathbf{P}$ as follows:

Proposition 3.10. *Suppose* $\mathbf{U}$, $\mathbf{V}$ *and* $\mathbf{W}$ *satisfy (11), (12) and (15). Then*

$$\begin{aligned}
\bar{\mathbf{U}} &= \mathbf{U} - \frac{1}{m_x}\Sigma_n\Sigma'_{m_x}\left(E'_x\mathbf{U} - \mathbf{U}_0\right),\\
\bar{\mathbf{V}} &= \mathbf{V} - \frac{1}{m_y}\Sigma_n\Sigma'_{m_y}\left(E'_y\mathbf{V} - \mathbf{V}_0\right),\\
\bar{\mathbf{W}} &= \mathbf{W} - \frac{1}{m_z}\Sigma_n\Sigma'_{m_z}\left(E'_z\mathbf{W} - \mathbf{V}_0\right),\\
\bar{\mathbf{P}} &= \mathbf{P}
\end{aligned}$$

satisfiy (11), (12) and (13).

Proof. Since $\bar{\mathbf{U}}$ and $\mathbf{U}$ differ only by a constant, $\bar{\mathbf{U}}$ inherits the validity of (11) and (12) from $\mathbf{U}$ because the difference operators vanish on constant vectors.

We prove the statement only for the first component of velocity, the other two components are proven analoguously.

We begin with (15):

$$\begin{aligned}
P'_{m_x}E'_x\mathbf{U} &= P'_{m_x}\mathbf{U}_0\\
\left(I(m_x) - \frac{1}{m_x}\Sigma_n\Sigma'_{m_x}\right)E'_x\mathbf{U} &= \left(I(m_x) - \frac{1}{m_x}\Sigma_n\Sigma'_{m_x}\right)\mathbf{U}_0\\
I(m_x)\left(E'_x\mathbf{U} - \mathbf{U}_0\right) &= \frac{1}{m_x}\Sigma_n\Sigma'_{m_x}\left(E'_x\mathbf{U} - \mathbf{U}_0\right).
\end{aligned}$$

This implies

$$E'_x\mathbf{U} = \mathbf{U}_0 + \mathbf{c},$$

where $\mathbf{c} = (c, c, \ldots, c) \in \mathbf{R}$ with

$$\mathbf{c} = \frac{1}{m_x}\Sigma'_{m_x}\left(E'_x\mathbf{U} - \mathbf{U}_0\right).$$

Noting that

$$\mathbf{c} = E'_x\Sigma_n c,$$

we get

$$E'_x\left(\mathbf{U} - \frac{1}{m_x}\Sigma'_n\Sigma_{m_x}\left(E'_x\mathbf{U} - \mathbf{U}_0\right)\right) = \mathbf{U}_0. \tag{16}$$

In (13), $\mathbf{U}_0 = \mathbf{O}_{m_x}$, $\mathbf{V}_0 = \mathbf{O}_{m_y}$ and $\mathbf{W}_0 = \mathbf{O}_{m_z}$, $\bar{\mathbf{U}}$, $\bar{\mathbf{V}}$ and $\bar{\mathbf{W}}$ simplify to

$$\begin{aligned}\bar{\mathbf{U}} &= \mathbf{U} - \frac{1}{m_x}\Sigma_n'\Sigma_{m_x}E_x'\mathbf{U},\\ \bar{\mathbf{V}} &= \mathbf{V} - \frac{1}{m_y}\Sigma_n'\Sigma_{m_y}E_y'\mathbf{V},\\ \bar{\mathbf{W}} &= \mathbf{W} - \frac{1}{m_z}\Sigma_n'\Sigma_{m_z}E_z'\mathbf{W}.\end{aligned}$$

So (16) simplifies to

$$E_x'\left(\mathbf{U} - \frac{1}{m_x}\Sigma_n'\Sigma_{m_x}\left(E_x'\mathbf{U}\right)\right) = \mathbf{O}_{m_x},$$

which is (13) for $\bar{\mathbf{U}}$ from the proposition for $\mathbf{U}_0 = \mathbf{O}_{m_x}$. □

By applying the discrete divergence operator to the three equations (11), using that $D_x^+\Delta_h = \Delta_h D_x^+$, $D_y^+\Delta_h = \Delta_h D_y^+$, $D_z^+\Delta_h = \Delta_h D_z^+$ and using (12) we get

$$\Delta_h\mathbf{P} = \left(D_x^+\Psi_x\mathbf{F}_x + D_y^+\Psi_y\mathbf{F}_y + D_z^+\Psi_z\mathbf{F}_z\right) + \left(D_x^+\bar{\mathbf{F}}_x + D_y^+\bar{\mathbf{F}}_y + D_z^+\bar{\mathbf{F}}_z\right). \tag{17}$$

Now we have the notation for a 7×7 block system that discretizes the Stokes equations and the jump equations explicitly: Define

$$M = \left[\begin{array}{ccc|c|ccc} \Delta_h & \mathcal{O} & \mathcal{O} & -D_x^- & \Psi_x & \mathcal{O} & \mathcal{O}\\ \mathcal{O} & \Delta_h & \mathcal{O} & -D_y^- & \mathcal{O} & \Psi_y & \mathcal{O}\\ \mathcal{O} & \mathcal{O} & \Delta_h & -D_z^- & \mathcal{O} & \mathcal{O} & \Psi_z\\ \hline \mathcal{O} & \mathcal{O} & \mathcal{O} & \Delta_h & -D_x^+\Psi_x & -D_y^+\Psi_y & -D_z^+\Psi_z\\ \hline \Psi_x' & \mathcal{O} & \mathcal{O} & \mathcal{O} & \mathcal{O} & \mathcal{O} & \mathcal{O}\\ \mathcal{O} & \Psi_y' & \mathcal{O} & \mathcal{O} & \mathcal{O} & \mathcal{O} & \mathcal{O}\\ \mathcal{O} & \mathcal{O} & \Psi_z' & \mathcal{O} & \mathcal{O} & \mathcal{O} & \mathcal{O} \end{array}\right],$$

$$\mathbf{X} = \begin{bmatrix}\mathbf{U}\\ \mathbf{V}\\ \mathbf{W}\\ \mathbf{P}\\ \mathbf{F}_x\\ \mathbf{F}_y\\ \mathbf{F}_z\end{bmatrix}, \mathbf{B} = \begin{bmatrix}-\bar{\mathbf{F}}_x\\ -\bar{\mathbf{F}}_y\\ -\bar{\mathbf{F}}_z\\ D_x^+\bar{\mathbf{F}}_x + D_y^+\bar{\mathbf{F}}_y + D_z^+\bar{\mathbf{F}}_z\\ \mathbf{O}_{m_x}\\ \mathbf{O}_{m_y}\\ \mathbf{O}_{m_z}\end{bmatrix}$$

then we need to solve

$$M\mathbf{X} = \mathbf{B}. \tag{18}$$

Theorem 3.11. *Let* $\mathbf{X}$ *be a solution of (18), with first four blocks* $\mathbf{U}$, $\mathbf{V}$, $\mathbf{W}$ *and* $\mathbf{P}$. *Define* $\bar{\mathbf{U}}$, $\bar{\mathbf{V}}$ *and* $\bar{\mathbf{W}}$ *as in Proposition 3.10. Then the restriction of* $\bar{\mathbf{U}}$, $\bar{\mathbf{V}}$, $\bar{\mathbf{W}}$ *and* $\mu\bar{\mathbf{P}} = \mu\mathbf{P}$ *to* $\Omega\setminus G$ *solves (8) — (10).*

Proof. By construction, the orignal equations (8) – (10) are a subset of the equations (11) – (13). Hence any solution of (11) – (13), when restricted to $\Omega\setminus G$ also solves (8) – (10). Since (17) implies (12) by contradiction, the claim follows by Proposition 3.10. □

4. Schur-complement formulation

4.1. **Elimination of the pressure.** By construction, the right hand side in (17) is always in $\mathbf{R}^n \setminus S_n$. Thus (17) can alwys be solved for P by applying the supspace inverse $\Delta_h^\dagger$ via FFT:

$$(\mathcal{F}P)_{l,m,p} = \frac{h^2\,(\mathcal{F}F)_{l,m,p}}{\left\{2\cos\left(\frac{2k\pi}{n_x}\right)+2\cos\left(\frac{2m\pi}{n_y}\right)+2\cos\left(\frac{2p\pi}{n_z p}\right)-6\right\}}$$

with $(\mathcal{F}P)_{0,0,0}=0$ as in Proposition 3.8.

Using the subspace inverse $\Delta_h^\dagger$, the pressure can be eliminated from (18). The pressure is split into two parts, the component resulting from the application of $\Delta_h^\dagger$ to the 4th block of the right hand side B and the application of $\Delta_h^\dagger$ to the fictitious forces. This provides the notation for an efficient method to solve (11), (12) and (14).

$$\begin{aligned} P &= P_1 + P_2, \\ P_1 &= \Delta_h^\dagger\left(D_x^+\Psi_x\mathbf{F}_x + D_y^+\Psi_y\mathbf{F}_y + D_z^+\Psi_z\mathbf{F}_z\right), \\ P_2 &= \Delta_h^\dagger\left(D_x^+\bar{\mathbf{F}}_x + D_y^+\bar{\mathbf{F}}_y + D_z^+\bar{\mathbf{F}}_z\right). \end{aligned}$$

The resulting Schur-complement is

$$M_1\begin{bmatrix} U \\ V \\ W \\ \mathbf{F}_x \\ \mathbf{F}_y \\ \mathbf{F}_z \end{bmatrix} = \begin{bmatrix} -\bar{\mathbf{F}}_x + D_x^- P_2 \\ -\bar{\mathbf{F}}_y + D_y^- P_2 \\ -\bar{\mathbf{F}}_z + D_z^- P_2 \\ O_{m_x} \\ O_{m_y} \\ O_{m_z} \end{bmatrix},$$

where

$$M_1 = \left[\begin{array}{ccc|ccc} \Delta_h & \mathcal{O} & \mathcal{O} & \left(I - D_x^-\Delta_h^\dagger D_x^+\right)\Psi_x & -D_x^-\Delta_h^\dagger D_y^+\Psi_y & -D_x^-\Delta_h^\dagger D_z^+\Psi_z \\ \mathcal{O} & \Delta_h & \mathcal{O} & -D_y^-\Delta_h^\dagger D_x^+\Psi_x & \left(I - D_y^-\Delta_h^\dagger D_y^+\right)\Psi_y & -D_y^-\Delta_h^\dagger D_z^+\Psi_z \\ \mathcal{O} & \mathcal{O} & \Delta_h & -D_z^-\Delta_h^\dagger D_x^+\Psi_x & -D_z^-\Delta_h^\dagger D_y^+\Psi_y & \left(I - D_z^-\Delta_h^\dagger D_z^+\right)\Psi_z \\ \hline \Psi_x' & \mathcal{O} & \mathcal{O} & \mathcal{O} & \mathcal{O} & \mathcal{O} \\ \mathcal{O} & \Psi_y' & \mathcal{O} & \mathcal{O} & \mathcal{O} & \mathcal{O} \\ \mathcal{O} & \mathcal{O} & \Psi_z' & \mathcal{O} & \mathcal{O} & \mathcal{O} \end{array}\right].$$

4.2. **Elimination of the velocities.** Similar to the elimination of P, (11) can always be solved for U, V and W because each of the 4 terms in each of the three sets of equations lies in $\mathbf{R}^n \setminus S_n$. Each component of velocity is split into two parts, the component resulting from the application of $\Delta_h^\dagger$ to the first, second and third block of the right hand side B and the application of $\Delta_h^\dagger$ to the terms involving the fictitious

forces.

$$\begin{aligned}
U &= U_1 + U_2, \\
U_1 &= \Delta_h^\dagger \left(\left(-I + D_x^- \Delta_h^\dagger D_x^+ \right) \Psi_x \mathbf{F}_x + D_x^- \Delta_h^\dagger D_y^+ \Psi_y \mathbf{F}_y + D_x^- \Delta_h^\dagger D_z^+ \Psi_z \mathbf{F}_z \right), \\
U_2 &= \Delta_h^\dagger \left(D_x^- P_2 - \bar{\mathbf{F}}_x \right), \\
V &= V_1 + V_2, \\
V_1 &= \Delta_h^\dagger \left(D_y^- \Delta_h^\dagger D_x^+ \Psi_x \mathbf{F}_x + \left(-I + D_y^- \Delta_h^\dagger D_y^+ \right) \Psi_y \mathbf{F}_y + D_y^- \Delta_h^\dagger D_z^+ \Psi_z \mathbf{F}_z \right), \\
V_2 &= \Delta_h^\dagger \left(D_y^- P_2 - \bar{\mathbf{F}}_y \right), \\
W &= W_1 + W_2, \\
W_1 &= \Delta_h^\dagger \left(D_z^- \Delta_h^\dagger D_x^+ \Psi_x \mathbf{F}_x + D_z^- \Delta_h^\dagger D_y^+ \Psi_y \mathbf{F}_y + \left(-I + D_z^- \Delta_h^\dagger D_z^+ \right) \Psi_z \mathbf{F}_z \right), \\
W_2 &= \Delta_h^\dagger \left(D_z^- P_2 - \bar{\mathbf{F}}_z \right).
\end{aligned}$$

Again we have split U, V and W into repeating and one-time calculations as to provide the notation for an efficient method to solve (11), (12) and (14).

This Schur-complement is the final set of equations on ∂G that is solved numerically:

$$M_2 \begin{bmatrix} \mathbf{F}_x \\ \mathbf{F}_y \\ \mathbf{F}_z \end{bmatrix} = - \begin{bmatrix} \Psi_x' U_2 \\ \Psi_y' V_2 \\ \Psi_z' W_2 \end{bmatrix}, \tag{19}$$

where

$$M_2 = \begin{bmatrix} \Psi_x' \Delta_h^\dagger \left(-I + D_x^- \Delta_h^\dagger D_x^+ \right) \Psi_x & \Psi_x' \Delta_h^\dagger D_x^- \Delta_h^\dagger D_y^+ \Psi_y & \Psi_x' \Delta_h^\dagger D_x^- \Delta_h^\dagger D_z^+ \Psi_z \\ \Psi_y' \Delta_h^\dagger D_y^- \Delta_h^\dagger D_x^+ \Psi_x & \Psi_y' \Delta_h^\dagger \left(-I + D_y^- \Delta_h^\dagger D_y^+ \right) \Psi_y & \Psi_y' \Delta_h^\dagger D_y^- \Delta_h^\dagger D_z^+ \Psi_z \\ \Psi_z' \Delta_h^\dagger D_z^- \Delta_h^\dagger D_x^+ \Psi_x & \Psi_z' \Delta_h^\dagger D_z^- \Delta_h^\dagger D_y^+ \Psi_y & \Psi_z' \Delta_h^\dagger \left(-I + D_z^- \Delta_h^\dagger D_z^+ \right) \Psi_z \end{bmatrix}.$$

Proposition 4.1. *M_2 is symmetric.*

Proof. This follows from the facts that $\Delta_h^\dagger$ is symmetric, $D_x^+ = -D_x^{-\prime}$, $D_y^+ = -D_y^{-\prime}$, $D_z^+ = -D_z^{-\prime}$ and because the one-sided differences $D_x^-, D_y^-, D_z^-, D_x^+, D_y^+$ and D_z^+ commute with $\Delta_h^\dagger$, by Proposition 3.5 and Proposition 3.6. □

Remark 4.1. *After (19) is solved for $\mathbf{F}_x$, $\mathbf{F}_y$ and $\mathbf{F}_z$, the solution of the original problem is found by adding known vectors and restricting them to the original domain*

$$\begin{aligned}
U &= (U_1 + U_2)|_{\Omega \setminus G}, \\
V &= (V_1 + V_2)|_{\Omega \setminus G}, \\
W &= (W_1 + W_2)|_{\Omega \setminus G}, \\
P &= \mu \, (P_1 + P_2)|_{\Omega \setminus G}.
\end{aligned}$$

Remark 4.2. *The Schur-complement system (19) inherits the non-trivial null-space from the extended system. Only the dimension is reduced by 4, one dimension per eliminated set of variables U, V, W and P:*

$$dim\ \mathcal{N} \approx 3 + max(\#S - \#F, 1),$$

with notation as in Remark 3.4.

To cope with this indefiniteness of the matrix, we follow the advice in [1] *and use* `MINRES` [15] *rather than* `CG`*.*

4.3. **Efficient Schur-complement multiplication.** To solve (19) with conjugate gradients, the matrix-vector product on the left of (19) must be evaluated. This can be done very efficiently as follows. First, auxiliary vectors of projected embedded forces are computed:

$$\tilde{\mathbf{F}}_x = \Psi_x \mathbf{F}_x, \tilde{\mathbf{F}}_y = \Psi_y \mathbf{F}_y, \tilde{\mathbf{F}}_z = \Psi_z \mathbf{F}_z.$$

Baed on these quantities, in every matrix-vector product evaluation, exactly 4 Poisson problems must be solved:

$$\begin{aligned} P_1 &= \Delta_h^\dagger \left(D_x^+ \tilde{\mathbf{F}}_x + D_y^+ \tilde{\mathbf{F}}_y + D_z^+ \tilde{\mathbf{F}}_z \right), \\ U_1 &= \Delta_h^\dagger \left(D_x^- P_1 - \tilde{\mathbf{F}}_x \right), \\ V_1 &= \Delta_h^\dagger \left(D_y^- P_1 - \tilde{\mathbf{F}}_y \right), \\ W_1 &= \Delta_h^\dagger \left(D_z^- P_1 - \tilde{\mathbf{F}}_z \right), \end{aligned}$$

and finally the matrix-vector product

$$M_2 \begin{bmatrix} \mathbf{F}_x \\ \mathbf{F}_y \\ \mathbf{F}_z \end{bmatrix} \text{ in (19) can be quickly evaluated as } \begin{bmatrix} \Psi_x' U_1 \\ \Psi_y' V_1 \\ \Psi_z' W_1 \end{bmatrix}.$$

Proposition 4.2. *The arguments in the computation of P_1, U_1, V_1 and W_1 satisfy (7), i.e. they are in the range S_n of the operator $\Delta_h^\dagger$ for any $\mathbf{F}_x \in \mathbf{R}^{m_x}$, $\mathbf{F}_y \in \mathbf{R}^{m_y}$ and $\mathbf{F}_z \in \mathbf{R}^{m_z}$.*

Proof. $\tilde{\mathbf{F}}_x \in S_n$ by definition of Ψ_x, and similarly $\tilde{\mathbf{F}}_y$ and $\tilde{\mathbf{F}}_z$. Similarly, by the definition of D_x^+, D_x^-, D_y^+, D_y^-, D_z^+ and D_z^-, $D_x^+ \tilde{\mathbf{F}}_x \in S_n$, $D_y^+ \tilde{\mathbf{F}}_y \in S_n$, $D_z^+ \tilde{\mathbf{F}}_z \in S_n$, $D_x^- P_1 \in S_n$, $D_y^- P_1 \in S_n$ and $D_z^- P_1 \in S_n$. Since the sum of elements in S_n is again in S_n the proof is complete. □

5. Examples

The method is already in use in many ongoing projects, mostly regarding the virtual material design of so-called nonwoven [20], for the purpose of filtration simulations [18], fuel cell simulations [21] and simulations of paper dewatering felts.

5.1. Example 1: permeability of a unit cell with spherical obstacles.

5.1.1. *Results for permeability.* Jung and Torquato [10] considered the unit cell with spherical obstacles of various diameters to valiate their computed permeability against solutions by Sangani and Acrivos [19].

We will also consider these values from [19] as the correct solution.

Spherical obstacles are placed at the center of the unit cell. The diameter of the obstacle is varied from 0.1 to 1, and the computed permeabilty of the resulting cell is listed in Table 1.

$\chi \vert N$	40	80	160	240	J&T [10]	S&A [19]
0.1	$10.15e^{-1}$ (4/7/1.0)	$9.245e^{-1}$ (15/48/9.6)	$9.182e^{-1}$ (26/413/131)	$9.220e^{-1}$ (30/1389/482)	$9.147e^{-1}$	$9.112e^{-1}$
0.2	$3.902e^{-1}$ (15/8/1.3)	$3.836e^{-1}$ (26/53/14)	$3.844e^{-1}$ (36/414/169)	$3.847e^{-1}$ (42/1393/633)	$3.844e^{-1}$	$3.822e^{-1}$
0.3	$2.136e^{-1}$ (21/7/1.5)	$2.105e^{-1}$ (31/51/16)	$2.097e^{-1}$ (41/418/187)	$2.092e^{-1}$ (48/1405/710)	$2.107e^{-1}$	$2.081e^{-1}$
0.4	$1.249e^{-1}$ (26/8/1.7)	$1.238e^{-1}$ (35/51/17)	$1.240e^{-1}$ (44/425/200)	$1.239e^{-1}$ (53/1425/766)	$1.252e^{-1}$	$1.233e^{-1}$
0.5	$7.622e^{-2}$ (26/8/1.7)	$7.524e^{-2}$ (36/54/18)	$7.524e^{-2}$ (44/435/199)	$7.505e^{-2}$ (52/1458/768)	$7.638e^{-2}$	$7.467e^{-2}$
0.6	$4.622e^{-2}$ (27/8/1.7)	$4.508e^{-2}$ (36/54/18)	$4.488e^{-2}$ (44/450/200)	$4.476e^{-2}$ (50/1504/742)	$4.580e^{-2}$	$4.450e^{-2}$
0.7	$2.619e^{-2}$ (27/9/1.7)	$2.558e^{-2}$ (34/57/17)	$2.550e^{-2}$ (42/470/192)	$2.543e^{-2}$ (47/1568/705)	$2.606e^{-2}$	$2.525e^{-2}$
0.8	$1.372e^{-2}$ (27/10/1.7)	$1.345e^{-2}$ (33/61/17)	$1.335e^{-2}$ (41/496/188)	$1.331e^{-2}$ (47/1652/695)	$1.376e^{-2}$	$1.320e^{-2}$
0.85	$9.617e^{-3}$ (28/10/1.7)	$9.346e^{-3}$ (33/63/17)	$9.292e^{-3}$ (41/512/189)	$9.250e^{-3}$ (47/1653/697)	$9.596e^{-3}$	$9.152e^{-3}$
0.9	$6.548e^{-3}$ (27/10/1.7)	$6.350e^{-3}$ (34/66/17)	$6.257e^{-3}$ (42/529/193)	$6.227e^{-3}$ (47/1758/698)	$6.480e^{-3}$	$6.153e^{-3}$
0.95	$4.354e^{-3}$ (28/11/1.8)	$4.115e^{-3}$ (36/68/18)	$4.068e^{-3}$ (43/548/198)	$4.050e^{-3}$ (49/1820/736)	$4.247e^{-3}$	$4.003e^{-3}$
1.0	$2.692e^{-3}$ (31/11/1.8)	$2.611e^{-3}$ (36/71/18)	$2.573e^{-3}$ (46/569/209)	$2.555e^{-3}$ (54/1888/799)	$2.673e^{-3}$	$2.520e^{-3}$

TABLE 1. Permeabilities, iteration counts, memory (MB) and run times (seconds) for example 1.

The small print in the parentheses in Table 1 indicates the number of iterations required and the required run time in seconds. Even on the coarsest grid, the permeabilities already give the correct impression when compared to [19]. The computed permeabilities are not monotone under grid refinement. This may be explained by the fact that the two finest grids are not nested, because we wanted to keep the computations feasible on a computer with 2GB memory. Otherwise, our uniform grid computations yield better results than [10] for the larger spheres and slightly worse than [10] for the smallest sphere. This is explained by a discussion in [10] that the smaller the sphere, the lower the quality of the representation on a fixed grid. This is graphed in Figure 3, here relative errors are plottetd. Both approaches always overestimate the permeability. In the case of FFF-Stokes it is due to the fact that the boundary conditions in the tangential direction are enforced half a voxel inside the

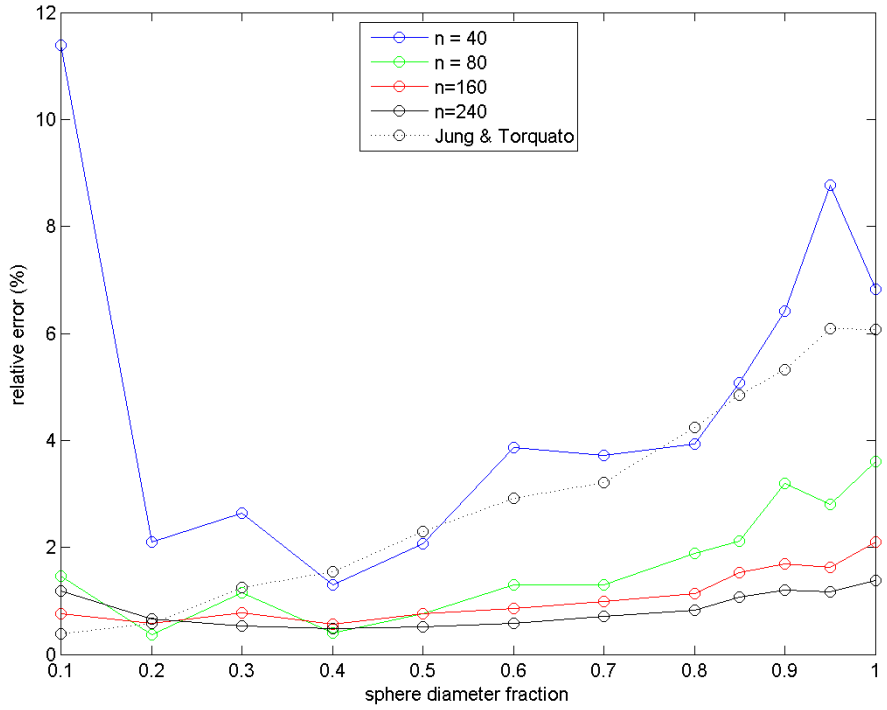

FIGURE 3. *Plot of the relative error in the data in Table 1. First order of FFF-Stokes is visible as well as the better values of Jung and Torquato* [10] *for small spheres. Both approaches consistently overestimate the permeability.*

solid, thus providing the flow solver with an effectivley larger emtpy region, where a higher permeability is expected.

Unfortunatley, [10] give no run time and memory requirements for their calculations. This is probably because their main interest was in providing numerical evidence that maximum fluid permeability of triply periodic porous structures with a simply connected pore space and 50% porosity is achieved by a structure that globally minimizes the specific surface.

The C++ code took between 1 second for the easiest 40^3 problem with about $256000 = 4 \times 40 \times 40 \times 40$ variables less than 17 minutes for the 240^3 problem with more than 55 million variables. Thus, the code may be a very useful tool for performing studies such as the one in [10].

5.1.2. *Convergence of the original variables.* The method works on reducing the residual of the Schur-complement system for the fictitious forces, but the real interest lies the quality of the solution in the original variables. This example illustrates that the reduction of the residual of the Schur-complement is also a meaningful criterion for the original variables.

Table 2 shows that the 2-norm of the differences between the velocities computed with 6 digits residual decrease of the Schur-complement and the velocities computed to 1, 2, 3, 4, and 5 digits, respectively, behave exactly the same as the Schur-complement variables. For the pressure the convergence is initially slower. Only on the finest grid the decrease is on the same order of magnitude as for the Schur-complement variables.

$\frac{\|\|\|r_G\|\|\|}{\|\|\|RHS\|\|\|}$	$\frac{\|\|\|U^i-U^6\|\|\|_2}{\|\|\|U^6\|\|\|_2}$	$\frac{\|\|\|V^i-V^6\|\|\|_2}{\|\|\|V^6\|\|\|_2}$	$\frac{\|\|\|W^i-W^6\|\|\|_2}{\|\|\|W^6\|\|\|_2}$	$\frac{\|\|P^i-P^6\|\|_2}{\|\|P^6\|\|_2}$	
1e-1	4.73e-01	1.44e-01	7.79e-01	3.63e-01	
1e-2	5.26e-02	1.87e-02	5.76e-02	1.08e-01	
1e-3	4.96e-03	1.97e-03	5.18e-03	3.40e-02	
1e-4	4.67e-04	2.10e-04	5.45e-04	1.15e-02	
1e-5	4.26e-05	1.90e-05	5.06e-05	1.10e-03	

TABLE 2. Convergence of the original variables

5.1.3. *Convergence of* `MINRES` *vs* `CG`. To illustrate the benefit of using `MINRES` compared wit `CG`, Table 3 shows the number of Schur-complement matrix-vector products needed by `MINRES` and `CG` in order to achieve a fixed reduction of the residual of the Schur- complement. This is a reasonable quality measure because both methods are started with the zero-vector as initial guess, and the norm of the initial residual is simply the norm of the right hand side, i.e. agrees for the two cases.

	`CG`	`MINRES`
1e-1	7	5
1e-2	29	19
1e-3	91	48
1e-4	323	131

TABLE 3. Iteration counts of `MINRES` vs `CG`.

This means that the higher accuracy required, the greater the benefit of using `MINRES`. In particular, the residue does not decrease monotonically when using CG, and the residuals vary significantly (3rd digit of the norm) after as few as 40 iterations even for small sized problems. This is probably due to the nontrivial nullspace of the matrix as explained in [14].

5.1.4. *Performance in terms of run time and memory.* Since the FFT is known to be most efficient for powers of 2, it is interesting to see how the overall method performs on different lengths of the paralellepiped. Table 4 shows results for edge lengths that are equal to a prime (127), a power of 2 (128), and the product of two primes (128 = 3*43). The required memory (here: for our C++ implementation, not the matlab code [30]) behaves as expected, with a moderate increase for the larger problem. And the time per iteration also behaves as expected, it is by about a factor 2 better for the power of 2. The reason why this is not worse lies in the fact that a 3-dimensional Fourier transform actually consists of many 1d transforms, and hence the order parameter for

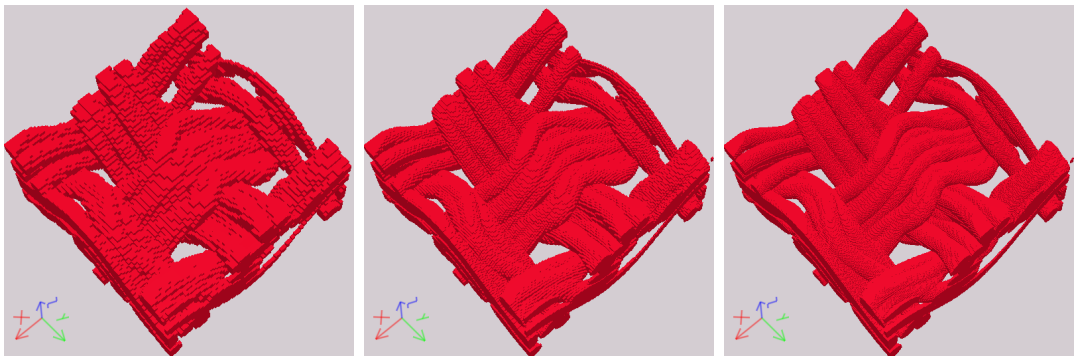

FIGURE 4. *3d view of of the plain weave cell with 10 filaments per thread. a)* $nx = 64$*, b)* $nx = 128$ *and c)* $nx = 256$*.*

the FFT is only n_x, n_y and n_z, respectively, and not the total number of variables $n = n_x \cdot n_y \cdot n_z$. Another reason is probably the quality of the FFTW implementation by Frigo and Johnson [5].

$n = 4n_xn_yn_z$	$n_x = n_y = n_z$	time / iteration (s)	memory (MB)
$8,193,532$	127	6.3	337
$8,388,608$	$2^7 = 128$	3.3	345
$8,586,756$	$3 * 43 = 129$	6.5	352

TABLE 4. Run time and memory for different prime factorizations

5.2. **Example 2: Permeabilities of multifilament woven textiles.**

5.2.1. *Resolution study.* As already illustrated in the first example, if only the permeability is needed, it is sufficient to work on rather coarse grids. Figure 4 and Table 5 illustrate this as follows: The same multifilament woven geometry is resolved with mesh width 1, 0.5 and 0.25. Then, flow in the z-direction is computed, and the mean flow velocity is listed in Table 5. As for the much simpler geometries in the first example, even for the coarse resolution the mean flow velocities are within 10% of the mean flow velocities computed on the mesh with the highest resolution. Considering that 10% is often a good assumption on the measurement error it follows that if the method works at all (agreement with measurements is the ultimate goal), then one might as well work with a very coarse grid.

nx	ny	nz	material	mean(u)	mean(v)	mean(w)
64	64	32	31%	-8.41e+03	-1.96e+04	1.66e+05
128	128	64	31%	-7.77e+03	-1.80e+04	1.56e+05
256	256	128	31%	-7.62e+03	-1.75e+04	1.52e+05

TABLE 5. Variation of velocity for 10 filament woven under grid refinement.

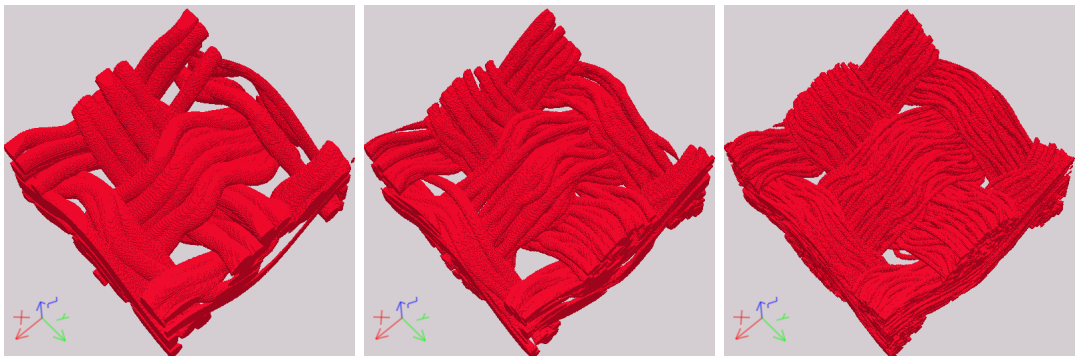

FIGURE 5. *3d view of of the plain weave cell a) 10 filaments per thread, b) 40 filaments per thread and c) 160 filaments per thread.*

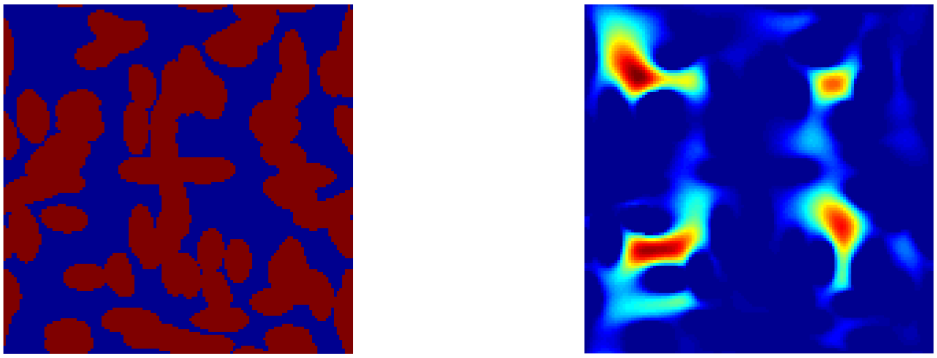

FIGURE 6. *Cross sections at the same in plane layer of the plain weave cell with a) structure and b) velocity magnitude.*

5.2.2. *Variation of filament diameter and number of filaments.* Given a fixed porosity and a fixed type of weaving pattern, the flow resistivity depends signifiantly on the number of filaments in a thread. Figure 5 and Table 6 illustrate this as follows: The same simple weaving pattern is used, with different numbers of filaments per thread. The filaments are made finer to keep the overall porosity. To resolve the thinnest filaments, we use the finest resolution from the previous example. Again the flow is in the z-direction, but now the mean flow velocity increases significantly for thicker and fewer filaments.

TABLE 6. varied number of filaments

nx	ny	nz	filaments	material	mean(u)	mean(v)	mean(w)
256	256	128	10	31%	-7.62e+03	-1.75e+04	1.52e+05
256	256	128	40	31%	7.78e+03	-2.08e+03	7.33e+04
256	256	128	160	31%	1.30e+02	-1.60e+02	2.23e+04

6. Remarks

Several features of FFF-Stokes are worth emphasizing:

(1) The inf-sup condition on the pressure is dealt with naturally by solving in Fourier space, where the constant is simply the first mode.
(2) The speed of convergence results from the fact that for highly porous media, the solution of forced free space (with force integrating to zero and periodic boundary conditions) is a good preconditioner for the problem with obstacles.
(3) The additional directions of null-space of the Schur-complement matrix are properly taken care of by using the `MINRES` variant of conjugate gradients.
(4) The speed of the implementation results from the fact that in this formulation almost all the work lies in the discrete Fourier transform, the free-space problem can be solved in $\mathcal{O}(n \log n)$. For the FFT, the very powerful FFTW implementation [5] is available in matlab and also as a C++ library.
(5) Notable are the low numbers of `MINRES` iterations required for the answer compared to results using `CG`.
(6) Another positive feature is the little increase in the required number of iterations under grid refinement. This is due to the fact that we stopped the solver after reducing the residual of the Schur-complement problem by 3 orders of magnitude. Control runs for an extra digit indicated that the permeability does not change anymore, and so one may stop the computations.
(7) It is an essential feature of FFF-Stokes that we have observed for all examples: It produces a solution that is correct to several digits extremely quickly and then takes more and more iterations for every extra digit. For permeability computations, this behavior is acceptable because usually only a couple digits can be measued in practice.

7. Conclusions

The permeability of porous media is estimated via the computation of Stokes flows in three-dimensional computer models of the micro structure of the media.

FFF-Stokes works directly on the voxel model without further need for meshing and thus provides a fast, memory efficient and easy-to-use tool to perform such permeability computations.

Great insights can be gained into the dependance of permeability on micro structure of real porous materials in diverse applications, such as filter, fuel cell and other materials. FFF-Stokes applies to virtual materials as well as real materials.

A matlab implementation is provided [30] to allow readers to experience the automation and speed of the method for realistic three-dimensional models.

One drawback of FFF-Stokes is a slow-down of convergence for higher accuracy and also for lower porosities.

The second, more relevant issue are large errors for narrow channels. Since the boundary condition in the tangential direction is enforced half a voxel inside the solid, the flow is too fast. This in general leads to an overestimation of the permeability. And if channels of 1 or a few voxels diameter are present, this error can be quite large.

Additionally, in these cases the good agreement of error in the Schur-complement residual and error in the original variables deteriorates.

Thus, we recommend FFF-Stokes for fairly open structures of porosities above 80%, where both accuracy and speed of solution are acceptable.

8. Acknowledgements

The author thanks the members of Fraunhofer ITWM's flow and complex structures department for countless helpful discussions on fluid dynamics, especially Stefan Rief for the final encouragement to finish the solver and Liping Cheng for first trying out the `MINRES` method.

Vita Rutka, Qing Zhang and Donatas Elvikis did much of the work implementing the C++ version and Lea K. Triebsch got her Masters degree [27] using an early (unsymmetric) version of FFF-Stokes.

This work could not have been done without the fast prototyping capabilities of Matlab and the amazing speed of the FFTW implementation [5] of the Fast Fourier Transform.

References

[1] R. Barrett, M. Berry, T. F. Chan, J. Demmel, J. Donato, J. Dongarra, V. Eijkhout, R. Pozo, C. Romine, and H. Van der Vorst. *Templates for the Solution of Linear Systems: Building Blocks for Iterative Methods, 2nd Edition*. SIAM, Philadelphia, PA, 1994.

[2] G. Biros, L. Ying, and D. Zorin. A fast solver for the stokes equations with distributed forces in complex geometries. *J. Comput. Phys.*, 193(1):317–348, 2003.

[3] A. Koponen et al. Permeability of Three-Dimensional Random Fiber Webs. *Physical Review Letters*, 80(4):716—719, 1998.

[4] E. A. Fadlun, R. Verzicco, P. Orlandi, and J. Mohd-Yusof. Combined immersed-boundary finite-difference methods for three-dimensional complex flow simulations. *J. Comp. Phys.*, 161:30–60, 2000.

[5] M. Frigo and S. G. Johnson. The Design and Implementation of FFTW3. *Proceedings of the IEEE*, 93(2):216–231, 2005. Special issue on "Program Generation, Optimization, and Platform Adaptation".

[6] D. Goldstein, R. Handler, and L. Sirovich. Modeling a no-slip flow boundary with an external force field. *J. Comp. Phys.*, 105:354–366, 1993.

[7] G. Golub, L. C. Huang, H. Simon, and W.-P. Tang. A fast Poisson solver for the finite difference solution of the incompressible Navier-Stokes equations. *SIAM J. Sci. Comput.*, 19(5):1606—1624, 1998.

[8] L. Helfen. *Investigation of the Structure, Formation and Properties of Porous, Cellular and Low-Density Materials with Synchrotron-Radiation Imaging*. PhD thesis, Fraunhofer Institut für zerstörungsfreie Prüfverfahren IZFP, Saarbrücken, 2005.

[9] K. Ito and J. Toivanen. Preconditioned iterative methods on sparse subspaces. *Applied Math. Lett.*, 19(11):1191—1197, 2006.

[10] Y. Jung and S. Torquato. Fluid permeabilities of triply periodic minimal surfaces. *Phys. Rev. E*, 72(056319), 2005.

[11] J. Kim, D. Kim, and H. Choi. An Immersed-Boundary Finite-Volume Method for Simulations of Flow in Complex Geometries. *J. Comp. Phys.*, 171:132–150, 2001.

[12] R. J. LeVeque and Z. Li. Immersed interface methods for Stokes flow with elastic boundaries or surface tension. *SIAM J. Sci. Comp.*, 18(3):709—735, 1997.

[13] J. Martikainen, T. Rossi, and J. Toivanen. A fast direct solver for elliptic problems with a divergence constraint. *Numerical Linear Algebra with Applications*, 9:629—652, 2002.

[14] C. Paige, B.N. Parlett, and H.A. van der Vorst. Approximate solutions and eigenvalue bounds from Krylov subspaces. *Numerical Linear Algebra with Applications*, 29:115—134, 1995.
[15] C. Paige and M. Saunders. Solution of Sparse Indefinite Systems of Linear Equations. *SIAM J. Numer. Anal.*, 12:617—629, 1975.
[16] C. S. Peskin. Numerical Analysis of Blood Flow in the Heart. *J. Comput. Phys.*, 25:220—252, 1977.
[17] W. Proskurowski and O. Widlund. On the Numerical Solution of Helmholtz's Equation by the Capacitance Matrix Method. *Math. Comp.*, 30(135):433—468, 1976.
[18] S. Rief, A. Latz, and A. Wiegmann. Computer simulation of air filtration including electric surface charges in three-dimensional fibrous micro structure. *Filtration*, 6(2):169—172, 2006.
[19] A. Sangani and A. Acrivos. Slow flow through a periodic array of spheres. *Int. J. Multiphase Flow*, 8:343–360, 1982.
[20] K. Schladitz, S. Peters, D. Reinel-Bitzer, A. Wiegmann, and J. Ohser. Design of acoustic trim based on geometric modeling and flow simulation for non-woven. *Comp. Mat. Sci.*, 38:56—66, 2006.
[21] V. Schulz, J. Becker, A. Wiegmann, P. Mukherjee, and C.-Y. Wang. Modelling of Two-phase Behaviour in the Gas Diffusion Medium of Polymer Electrolyte Fuel cells via Full Morphology Approach. *J. Electrochem. Soc.*, 154(4), 2007.
[22] V. Schulz, D. Kehrwald, A. Wiegmann, and K. Steiner. Flow, heat conductivity, and gas diffusion in partly saturated microstructures. In *NAFEMS Seminar: Simulation of Complex Flows (CFD)*, April 2005.
[23] P. N. Swarztrauber. The methods of cyclic reduction and Fourier analysis and the FACR algorithm for the discrete solution of Poisson's equation on a rectangle. *Siam Review*, 19:490—501, 1977.
[24] X. Thibault and J. F. Bloch. Structural Analysis by X-ray Microtomography of Strained Nonwoven Papermaker Felt. *Textile Research Journal*, 72(6):480–485, 2002.
[25] H. Thoemen, T. Walther, and A. Wiegmann. 3D simulation of the macroscopic heat and mass transfer properties from the microstructure of wood fibre networks. Submitted, April 2007.
[26] S. Torquato. *Random Heterogeneous Materials*. Springer: New York, 2002.
[27] L. K. Triebsch. A Discrete Boundary Integral Approach to 3D Cell problems with Complex Geometry. Master's thesis, Universität Kaiserslautern, 2001.
[28] Y.-H. Tseng and J. H.Ferziger. A ghost-cell immersed boundary method for flow in complex geometry. *J. Comp. Phys.*, 192:593–623, 2003.
[29] A. Wiegmann. Fast Poisson, fast Helmholtz and fast linear elastostatic solvers on rectangular parallelepipeds. Technical Report LBNL-43565, Lawrence Berkeley National Laboratory, MS 50A-1148, One Cyclotron Rd, Berkeley CA 94720, June 1999.
[30] A. Wiegmann. FFF-Stokes matlab code. www.geodict.com/StokesPaper, © 2001-2007.
[31] A. Wiegmann and A. Zemitis. EJ-HEAT: A Fast Explicit Jump harmonic averaging solver for the effective heat conductivity of composite materials. Technical Report 94, Fraunhofer ITWM Kaiserslautern, 2006.

Published reports of the Fraunhofer ITWM

The PDF-files of the following reports are available under:
www.itwm.fraunhofer.de/de/zentral__berichte/berichte

1. D. Hietel, K. Steiner, J. Struckmeier
A Finite - Volume Particle Method for Compressible Flows
(19 pages, 1998)

2. M. Feldmann, S. Seibold
Damage Diagnosis of Rotors: Application of Hilbert Transform and Multi-Hypothesis Testing
Keywords: Hilbert transform, damage diagnosis, Kalman filtering, non-linear dynamics
(23 pages, 1998)

3. Y. Ben-Haim, S. Seibold
Robust Reliability of Diagnostic Multi-Hypothesis Algorithms: Application to Rotating Machinery
Keywords: Robust reliability, convex models, Kalman filtering, multi-hypothesis diagnosis, rotating machinery, crack diagnosis
(24 pages, 1998)

4. F.-Th. Lentes, N. Siedow
Three-dimensional Radiative Heat Transfer in Glass Cooling Processes
(23 pages, 1998)

5. A. Klar, R. Wegener
A hierarchy of models for multilane vehicular traffic
Part I: Modeling
(23 pages, 1998)

Part II: Numerical and stochastic investigations
(17 pages, 1998)

6. A. Klar, N. Siedow
Boundary Layers and Domain Decomposition for Radiative Heat Transfer and Diffusion Equations: Applications to Glass Manufacturing Processes
(24 pages, 1998)

7. I. Choquet
Heterogeneous catalysis modelling and numerical simulation in rarified gas flows Part I: Coverage locally at equilibrium
(24 pages, 1998)

8. J. Ohser, B. Steinbach, C. Lang
Efficient Texture Analysis of Binary Images
(17 pages, 1998)

9. J. Orlik
Homogenization for viscoelasticity of the integral type with aging and shrinkage
(20 pages, 1998)

10. J. Mohring
Helmholtz Resonators with Large Aperture
(21 pages, 1998)

11. H. W. Hamacher, A. Schöbel
On Center Cycles in Grid Graphs
(15 pages, 1998)

12. H. W. Hamacher, K.-H. Küfer
Inverse radiation therapy planning - a multiple objective optimisation approach
(14 pages, 1999)

13. C. Lang, J. Ohser, R. Hilfer
On the Analysis of Spatial Binary Images
(20 pages, 1999)

14. M. Junk
On the Construction of Discrete Equilibrium Distributions for Kinetic Schemes
(24 pages, 1999)

15. M. Junk, S. V. Raghurame Rao
A new discrete velocity method for Navier-Stokes equations
(20 pages, 1999)

16. H. Neunzert
Mathematics as a Key to Key Technologies
(39 pages (4 PDF-Files), 1999)

17. J. Ohser, K. Sandau
Considerations about the Estimation of the Size Distribution in Wicksell's Corpuscle Problem
(18 pages, 1999)

18. E. Carrizosa, H. W. Hamacher, R. Klein, S. Nickel
Solving nonconvex planar location problems by finite dominating sets
Keywords: Continuous Location, Polyhedral Gauges, Finite Dominating Sets, Approximation, Sandwich Algorithm, Greedy Algorithm
(19 pages, 2000)

19. A. Becker
A Review on Image Distortion Measures
Keywords: Distortion measure, human visual system
(26 pages, 2000)

20. H. W. Hamacher, M. Labbé, S. Nickel, T. Sonneborn
Polyhedral Properties of the Uncapacitated Multiple Allocation Hub Location Problem
Keywords: integer programming, hub location, facility location, valid inequalities, facets, branch and cut
(21 pages, 2000)

21. H. W. Hamacher, A. Schöbel
Design of Zone Tariff Systems in Public Transportation
(30 pages, 2001)

22. D. Hietel, M. Junk, R. Keck, D. Teleaga
The Finite-Volume-Particle Method for Conservation Laws
(16 pages, 2001)

23. T. Bender, H. Hennes, J. Kalcsics, M. T. Melo, S. Nickel
Location Software and Interface with GIS and Supply Chain Management
Keywords: facility location, software development, geographical information systems, supply chain management
(48 pages, 2001)

24. H. W. Hamacher, S. A. Tjandra
Mathematical Modelling of Evacuation Problems: A State of Art
(44 pages, 2001)

25. J. Kuhnert, S. Tiwari
Grid free method for solving the Poisson equation
Keywords: Poisson equation, Least squares method, Grid free method
(19 pages, 2001)

26. T. Götz, H. Rave, D. Reinel-Bitzer, K. Steiner, H. Tiemeier
Simulation of the fiber spinning process
Keywords: Melt spinning, fiber model, Lattice Boltzmann, CFD
(19 pages, 2001)

27. A. Zemitis
On interaction of a liquid film with an obstacle
Keywords: impinging jets, liquid film, models, numerical solution, shape
(22 pages, 2001)

28. I. Ginzburg, K. Steiner
Free surface lattice-Boltzmann method to model the filling of expanding cavities by Bingham Fluids
Keywords: Generalized LBE, free-surface phenomena, interface boundary conditions, filling processes, Bingham viscoplastic model, regularized models
(22 pages, 2001)

29. H. Neunzert
»Denn nichts ist für den Menschen als Menschen etwas wert, was er nicht mit Leidenschaft tun kann«
Vortrag anlässlich der Verleihung des Akademiepreises des Landes Rheinland-Pfalz am 21.11.2001
Keywords: Lehre, Forschung, angewandte Mathematik, Mehrskalenanalyse, Strömungsmechanik
(18 pages, 2001)

30. J. Kuhnert, S. Tiwari
Finite pointset method based on the projection method for simulations of the incompressible Navier-Stokes equations
Keywords: Incompressible Navier-Stokes equations, Meshfree method, Projection method, Particle scheme, Least squares approximation
AMS subject classification: 76D05, 76M28
(25 pages, 2001)

31. R. Korn, M. Krekel
Optimal Portfolios with Fixed Consumption or Income Streams
Keywords: Portfolio optimisation, stochastic control, HJB equation, discretisation of control problems
(23 pages, 2002)

32. M. Krekel
Optimal portfolios with a loan dependent credit spread
Keywords: Portfolio optimisation, stochastic control, HJB equation, credit spread, log utility, power utility, non-linear wealth dynamics
(25 pages, 2002)

33. J. Ohser, W. Nagel, K. Schladitz
The Euler number of discretized sets – on the choice of adjacency in homogeneous lattices
Keywords: image analysis, Euler number, neighborhod relationships, cuboidal lattice
(32 pages, 2002)

34. I. Ginzburg, K. Steiner
Lattice Boltzmann Model for Free-Surface flow and Its Application to Filling Process in Casting
Keywords: Lattice Boltzmann models; free-surface phenomena; interface boundary conditions; filling processes; injection molding; volume of fluid method; interface boundary conditions; advection-schemes; upwind-schemes
(54 pages, 2002)

35. M. Günther, A. Klar, T. Materne, R. Wegener
Multivalued fundamental diagrams and stop and go waves for continuum traffic equations
Keywords: traffic flow, macroscopic equations, kinetic derivation, multivalued fundamental diagram, stop and go waves, phase transitions
(25 pages, 2002)

36. S. Feldmann, P. Lang, D. Prätzel-Wolters
Parameter influence on the zeros of network determinants
Keywords: Networks, Equicofactor matrix polynomials, Realization theory, Matrix perturbation theory
(30 pages, 2002)

37. K. Koch, J. Ohser, K. Schladitz
Spectral theory for random closed sets and estimating the covariance via frequency space
Keywords: Random set, Bartlett spectrum, fast Fourier transform, power spectrum
(28 pages, 2002)

38. D. d'Humières, I. Ginzburg
Multi-reflection boundary conditions for lattice Boltzmann models
Keywords: lattice Boltzmann equation, boudary condistions, bounce-back rule, Navier-Stokes equation
(72 pages, 2002)

39. R. Korn
Elementare Finanzmathematik
Keywords: Finanzmathematik, Aktien, Optionen, Portfolio-Optimierung, Börse, Lehrerweiterbildung, Mathematikunterricht
(98 pages, 2002)

40. J. Kallrath, M. C. Müller, S. Nickel
Batch Presorting Problems: Models and Complexity Results
Keywords: Complexity theory, Integer programming, Assigment, Logistics
(19 pages, 2002)

41. J. Linn
On the frame-invariant description of the phase space of the Folgar-Tucker equation
Key words: fiber orientation, Folgar-Tucker equation, injection molding
(5 pages, 2003)

42. T. Hanne, S. Nickel
A Multi-Objective Evolutionary Algorithm for Scheduling and Inspection Planning in Software Development Projects
Key words: multiple objective programming, project management and scheduling, software development, evolutionary algorithms, efficient set
(29 pages, 2003)

43. T. Bortfeld , K.-H. Küfer, M. Monz, A. Scherrer, C. Thieke, H. Trinkaus
Intensity-Modulated Radiotherapy - A Large Scale Multi-Criteria Programming Problem
Keywords: multiple criteria optimization, representative systems of Pareto solutions, adaptive triangulation, clustering and disaggregation techniques, visualization of Pareto solutions, medical physics, external beam radiotherapy planning, intensity modulated radiotherapy
(31 pages, 2003)

44. T. Halfmann, T. Wichmann
Overview of Symbolic Methods in Industrial Analog Circuit Design
Keywords: CAD, automated analog circuit design, symbolic analysis, computer algebra, behavioral modeling, system simulation, circuit sizing, macro modeling, differential-algebraic equations, index
(17 pages, 2003)

45. S. E. Mikhailov, J. Orlik
Asymptotic Homogenisation in Strength and Fatigue Durability Analysis of Composites
Keywords: multiscale structures, asymptotic homogenization, strength, fatigue, singularity, non-local conditions
(14 pages, 2003)

46. P. Domínguez-Marín, P. Hansen, N. Mladenovi´c , S. Nickel
Heuristic Procedures for Solving the Discrete Ordered Median Problem
Keywords: genetic algorithms, variable neighborhood search, discrete facility location
(31 pages, 2003)

47. N. Boland, P. Domínguez-Marín, S. Nickel, J. Puerto
Exact Procedures for Solving the Discrete Ordered Median Problem
Keywords: discrete location, Integer programming
(41 pages, 2003)

48. S. Feldmann, P. Lang
Padé-like reduction of stable discrete linear systems preserving their stability
Keywords: Discrete linear systems, model reduction, stability, Hankel matrix, Stein equation
(16 pages, 2003)

49. J. Kallrath, S. Nickel
A Polynomial Case of the Batch Presorting Problem
Keywords: batch presorting problem, online optimization, competetive analysis, polynomial algorithms, logistics
(17 pages, 2003)

50. T. Hanne, H. L. Trinkaus
knowCube for MCDM – Visual and Interactive Support for Multicriteria Decision Making
Key words: Multicriteria decision making, knowledge management, decision support systems, visual interfaces, interactive navigation, real-life applications.
(26 pages, 2003)

51. O. Iliev, V. Laptev
On Numerical Simulation of Flow Through Oil Filters
Keywords: oil filters, coupled flow in plain and porous media, Navier-Stokes, Brinkman, numerical simulation
(8 pages, 2003)

52. W. Dörfler, O. Iliev, D. Stoyanov, D. Vassileva
On a Multigrid Adaptive Refinement Solver for Saturated Non-Newtonian Flow in Porous Media
Keywords: Nonlinear multigrid, adaptive refinement, non-Newtonian flow in porous media
(17 pages, 2003)

53. S. Kruse
On the Pricing of Forward Starting Options under Stochastic Volatility
Keywords: Option pricing, forward starting options, Heston model, stochastic volatility, cliquet options
(11 pages, 2003)

54. O. Iliev, D. Stoyanov
Multigrid – adaptive local refinement solver for incompressible flows
Keywords: Navier-Stokes equations, incompressible flow, projection-type splitting, SIMPLE, multigrid methods, adaptive local refinement, lid-driven flow in a cavity
(37 pages, 2003)

55. V. Starikovicius
The multiphase flow and heat transfer in porous media
Keywords: Two-phase flow in porous media, various formulations, global pressure, multiphase mixture model, numerical simulation
(30 pages, 2003)

56. P. Lang, A. Sarishvili, A. Wirsen
Blocked neural networks for knowledge extraction in the software development process
Keywords: Blocked Neural Networks, Nonlinear Regression, Knowledge Extraction, Code Inspection
(21 pages, 2003)

57. H. Knaf, P. Lang, S. Zeiser
Diagnosis aiding in Regulation Thermography using Fuzzy Logic
Keywords: fuzzy logic,knowledge representation, expert system
(22 pages, 2003)

58. M. T. Melo, S. Nickel, F. Saldanha da Gama
Largescale models for dynamic multicommodity capacitated facility location
Keywords: supply chain management, strategic planning, dynamic location, modeling
(40 pages, 2003)

59. J. Orlik
Homogenization for contact problems with periodically rough surfaces
Keywords: asymptotic homogenization, contact problems
(28 pages, 2004)

60. A. Scherrer, K.-H. Küfer, M. Monz, F. Alonso, T. Bortfeld
IMRT planning on adaptive volume structures – a significant advance of computational complexity
Keywords: Intensity-modulated radiation therapy (IMRT), inverse treatment planning, adaptive volume structures, hierarchical clustering, local refinement, adaptive clustering, convex programming, mesh generation, multi-grid methods
(24 pages, 2004)

61. D. Kehrwald
Parallel lattice Boltzmann simulation of complex flows
Keywords: Lattice Boltzmann methods, parallel computing, microstructure simulation, virtual material design, pseudo-plastic fluids, liquid composite moulding
(12 pages, 2004)

62. O. Iliev, J. Linn, M. Moog, D. Niedziela, V. Starikovicius
On the Performance of Certain Iterative Solvers for Coupled Systems Arising in Discretization of Non-Newtonian Flow Equations
Keywords: Performance of iterative solvers, Preconditioners, Non-Newtonian flow
(17 pages, 2004)

63. R. Ciegis, O. Iliev, S. Rief, K. Steiner
On Modelling and Simulation of Different Regimes for Liquid Polymer Moulding
Keywords: Liquid Polymer Moulding, Modelling, Simulation, Infiltration, Front Propagation, non-Newtonian flow in porous media
(43 pages, 2004)

64. T. Hanne, H. Neu
Simulating Human Resources in Software Development Processes
Keywords: Human resource modeling, software process, productivity, human factors, learning curve
(14 pages, 2004)

65. O. Iliev, A. Mikelic, P. Popov
Fluid structure interaction problems in deformable porous media: Toward permeability of deformable porous media
Keywords: fluid-structure interaction, deformable porous media, upscaling, linear elasticity, stokes, finite elements
(28 pages, 2004)

66. F. Gaspar, O. Iliev, F. Lisbona, A. Naumovich, P. Vabishchevich
On numerical solution of 1-D poroelasticity equations in a multilayered domain
Keywords: poroelasticity, multilayered material, finite volume discretization, MAC type grid
(41 pages, 2004)

67. J. Ohser, K. Schladitz, K. Koch, M. Nöthe
Diffraction by image processing and its application in materials science
Keywords: porous microstructure, image analysis, random set, fast Fourier transform, power spectrum, Bartlett spectrum
(13 pages, 2004)

68. H. Neunzert
Mathematics as a Technology: Challenges for the next 10 Years
Keywords: applied mathematics, technology, modelling, simulation, visualization, optimization, glass processing, spinning processes, fiber-fluid interaction, trubulence effects, topological optimization, multicriteria optimization, Uncertainty and Risk, financial mathematics, Malliavin calculus, Monte-Carlo methods, virtual material design, filtration, bio-informatics, system biology
(29 pages, 2004)

69. R. Ewing, O. Iliev, R. Lazarov, A. Naumovich
On convergence of certain finite difference discretizations for 1D poroelasticity interface problems
Keywords: poroelasticity, multilayered material, finite volume discretizations, MAC type grid, error estimates
(26 pages,2004)

70. W. Dörfler, O. Iliev, D. Stoyanov, D. Vassileva
On Efficient Simulation of Non-Newtonian Flow in Saturated Porous Media with a Multigrid Adaptive Refinement Solver
Keywords: Nonlinear multigrid, adaptive renement, non-Newtonian in porous media
(25 pages, 2004)

71. J. Kalcsics, S. Nickel, M. Schröder
Towards a Unified Territory Design Approach – Applications, Algorithms and GIS Integration
Keywords: territory desgin, political districting, sales territory alignment, optimization algorithms, Geographical Information Systems
(40 pages, 2005)

72. K. Schladitz, S. Peters, D. Reinel-Bitzer, A. Wiegmann, J. Ohser
Design of acoustic trim based on geometric modeling and flow simulation for non-woven
Keywords: random system of fibers, Poisson line process, flow resistivity, acoustic absorption, Lattice-Boltzmann method, non-woven
(21 pages, 2005)

73. V. Rutka, A. Wiegmann
Explicit Jump Immersed Interface Method for virtual material design of the effective elastic moduli of composite materials
Keywords: virtual material design, explicit jump immersed interface method, effective elastic moduli, composite materials
(22 pages, 2005)

74. T. Hanne
Eine Übersicht zum Scheduling von Baustellen
Keywords: Projektplanung, Scheduling, Bauplanung, Bauindustrie
(32 pages, 2005)

75. J. Linn
The Folgar-Tucker Model as a Differetial Algebraic System for Fiber Orientation Calculation
Keywords: fiber orientation, Folgar–Tucker model, invariants, algebraic constraints, phase space, trace stability
(15 pages, 2005)

76. M. Speckert, K. Dreßler, H. Mauch, A. Lion, G. J. Wierda
Simulation eines neuartigen Prüfsystems für Achserprobungen durch MKS-Modellierung einschließlich Regelung
Keywords: virtual test rig, suspension testing, multibody simulation, modeling hexapod test rig, optimization of test rig configuration
(20 pages, 2005)

77. K.-H. Küfer, M. Monz, A. Scherrer, P. Süss, F. Alonso, A. S. A. Sultan, Th. Bortfeld, D. Craft, Chr. Thieke
Multicriteria optimization in intensity modulated radiotherapy planning
Keywords: multicriteria optimization, extreme solutions, real-time decision making, adaptive approximation schemes, clustering methods, IMRT planning, reverse engineering
(51 pages, 2005)

78. S. Amstutz, H. Andrä
A new algorithm for topology optimization using a level-set method
Keywords: shape optimization, topology optimization, topological sensitivity, level-set
(22 pages, 2005)

79. N. Ettrich
Generation of surface elevation models for urban drainage simulation
Keywords: Flooding, simulation, urban elevation models, laser scanning
(22 pages, 2005)

80. H. Andrä, J. Linn, I. Matei, I. Shklyar, K. Steiner, E. Teichmann
OPTCAST – Entwicklung adäquater Strukturoptimierungsverfahren für Gießereien Technischer Bericht (KURZFASSUNG)
Keywords: Topologieoptimierung, Level-Set-Methode, Gießprozesssimulation, Gießtechnische Restriktionen, CAE-Kette zur Strukturoptimierung
(77 pages, 2005)

81. N. Marheineke, R. Wegener
Fiber Dynamics in Turbulent Flows Part I: General Modeling Framework
Keywords: fiber-fluid interaction; Cosserat rod; turbulence modeling; Kolmogorov's energy spectrum; double-velocity correlations; differentiable Gaussian fields
(20 pages, 2005)

Part II: Specific Taylor Drag
Keywords: flexible fibers; k-ε turbulence model; fiber-turbulence interaction scales; air drag; random Gaussian aerodynamic force; white noise; stochastic differential equations; ARMA process
(18 pages, 2005)

82. C. H. Lampert, O. Wirjadi
An Optimal Non-Orthogonal Separation of the Anisotropic Gaussian Convolution Filter
Keywords: Anisotropic Gaussian filter, linear filtering, orientation space, nD image processing, separable filters
(25 pages, 2005)

83. H. Andrä, D. Stoyanov
Error indicators in the parallel finite element solver for linear elasticity DDFEM
Keywords: linear elasticity, finite element method, hierarchical shape functions, domain decom-position, parallel implementation, a posteriori error estimates
(21 pages, 2006)

84. M. Schröder, I. Solchenbach
Optimization of Transfer Quality in Regional Public Transit
Keywords: public transit, transfer quality, quadratic assignment problem
(16 pages, 2006)

85. A. Naumovich, F. J. Gaspar
On a multigrid solver for the three-dimensional Biot poroelasticity system in multilayered domains
Keywords: poroelasticity, interface problem, multigrid, operator-dependent prolongation
(11 pages, 2006)

86. S. Panda, R. Wegener, N. Marheineke
Slender Body Theory for the Dynamics of Curved Viscous Fibers
Keywords: curved viscous fibers; fluid dynamics; Navier-Stokes equations; free boundary value problem; asymptotic expansions; slender body theory
(14 pages, 2006)

87. E. Ivanov, H. Andrä, A. Kudryavtsev
Domain Decomposition Approach for Automatic Parallel Generation of Tetrahedral Grids
Key words: Grid Generation, Unstructured Grid, Delaunay Triangulation, Parallel Programming, Domain Decomposition, Load Balancing
(18 pages, 2006)

88. S. Tiwari, S. Antonov, D. Hietel, J. Kuhnert, R. Wegener
A Meshfree Method for Simulations of Interactions between Fluids and Flexible Structures
Key words: Meshfree Method, FPM, Fluid Structure Interaction, Sheet of Paper, Dynamical Coupling
(16 pages, 2006)

89. R. Ciegis , O. Iliev, V. Starikovicius, K. Steiner
Numerical Algorithms for Solving Problems of Multiphase Flows in Porous Media
Keywords: nonlinear algorithms, finite-volume method, software tools, porous media, flows
(16 pages, 2006)

90. D. Niedziela, O. Iliev, A. Latz
On 3D Numerical Simulations of Viscoelastic Fluids
Keywords: non-Newtonian fluids, anisotropic viscosity, integral constitutive equation
(18 pages, 2006)

91. A. Winterfeld
Application of general semi-infinite Programming to Lapidary Cutting Problems
Keywords: large scale optimization, nonlinear programming, general semi-infinite optimization, design centering, clustering
(26 pages, 2006)

92. J. Orlik, A. Ostrovska
Space-Time Finite Element Approximation and Numerical Solution of Hereditary Linear Viscoelasticity Problems
Keywords: hereditary viscoelasticity; kern approximation by interpolation; space-time finite element approximation, stability and a priori estimate
(24 pages, 2006)

93. V. Rutka, A. Wiegmann, H. Andrä
EJIIM for Calculation of effective Elastic Moduli in 3D Linear Elasticity
Keywords: Elliptic PDE, linear elasticity, irregular domain, finite differences, fast solvers, effective elastic moduli
(24 pages, 2006)

94. A. Wiegmann, A. Zemitis
EJ-HEAT: A Fast Explicit Jump Harmonic Averaging Solver for the Effective Heat Conductivity of Composite Materials
Keywords: Stationary heat equation, effective thermal conductivity, explicit jump, discontinuous coefficients, virtual material design, microstructure simulation, EJ-HEAT
(21 pages, 2006)

95. A. Naumovich
On a finite volume discretization of the three-dimensional Biot poroelasticity system in multilayered domains
Keywords: Biot poroelasticity system, interface problems, finite volume discretization, finite difference method
(21 pages, 2006)

96. M. Krekel, J. Wenzel
A unified approach to Credit Default Swaption and Constant Maturity Credit Default Swap valuation
Keywords: LIBOR market model, credit risk, Credit Default Swaption, Constant Maturity Credit Default Swap-method
(43 pages, 2006)

97. A. Dreyer
Interval Methods for Analog Circiuts
Keywords: interval arithmetic, analog circuits, tolerance analysis, parametric linear systems, frequency response, symbolic analysis, CAD, computer algebra
(36 pages, 2006)

98. N. Weigel, S. Weihe, G. Bitsch, K. Dreßler
Usage of Simulation for Design and Optimization of Testing
Keywords: Vehicle test rigs, MBS, control, hydraulics, testing philosophy
(14 pages, 2006)

99. H. Lang, G. Bitsch, K. Dreßler, M. Speckert
Comparison of the solutions of the elastic and elastoplastic boundary value problems
Keywords: Elastic BVP, elastoplastic BVP, variational inequalities, rate-independency, hysteresis, linear kinematic hardening, stop- and play-operator
(21 pages, 2006)

100. M. Speckert, K. Dreßler, H. Mauch
MBS Simulation of a hexapod based suspension test rig
Keywords: Test rig, MBS simulation, suspension, hydraulics, controlling, design optimization
(12 pages, 2006)

101. S. Azizi Sultan, K.-H. Küfer
A dynamic algorithm for beam orientations in multicriteria IMRT planning
Keywords: radiotherapy planning, beam orientation optimization, dynamic approach, evolutionary algorithm, global optimization
(14 pages, 2006)

102. T. Götz, A. Klar, N. Marheineke, R. Wegener
A Stochastic Model for the Fiber Lay-down Process in the Nonwoven Production
Keywords: fiber dynamics, stochastic Hamiltonian system, stochastic averaging
(17 pages, 2006)

103. Ph. Süss, K.-H. Küfer
Balancing control and simplicity: a variable aggregation method in intensity modulated radiation therapy planning
Keywords: IMRT planning, variable aggregation, clustering methods
(22 pages, 2006)

104. A. Beaudry, G. Laporte, T. Melo, S. Nickel
Dynamic transportation of patients in hospitals
Keywords: in-house hospital transportation, dial-a-ride, dynamic mode, tabu search
(37 pages, 2006)

105. Th. Hanne
Applying multiobjective evolutionary algorithms in industrial projects
Keywords: multiobjective evolutionary algorithms, discrete optimization, continuous optimization, electronic circuit design, semi-infinite programming, scheduling
(18 pages, 2006)

106. J. Franke, S. Halim
Wild bootstrap tests for comparing signals and images
Keywords: wild bootstrap test, texture classification, textile quality control, defect detection, kernel estimate, nonparametric regression
(13 pages, 2007)

107. Z. Drezner, S. Nickel
Solving the ordered one-median problem in the plane
Keywords: planar location, global optimization, ordered median, big triangle small triangle method, bounds, numerical experiments
(21 pages, 2007)

108. Th. Götz, A. Klar, A. Unterreiter, R. Wegener
Numerical evidance for the non-existing of solutions of the equations desribing rotational fiber spinning
Keywords: rotational fiber spinning, viscous fibers, boundary value problem, existence of solutions
(11 pages, 2007)

109. Ph. Süss, K.-H. Küfer
Smooth intensity maps and the Bortfeld-Boyer sequencer
Keywords: probabilistic analysis, intensity modulated radiotherapy treatment (IMRT), IMRT plan application, step-and-shoot sequencing
(8 pages, 2007)

110. E. Ivanov, O. Gluchshenko, H. Andrä, A. Kudryavtsev
Parallel software tool for decomposing and meshing of 3d structures
Keywords: a-priori domain decomposition, unstructured grid, Delaunay mesh generation
(14 pages, 2007)

111. O. Iliev, R. Lazarov, J. Willems
Numerical study of two-grid preconditioners for 1d elliptic problems with highly oscillating discontinuous coefficients
Keywords: two-grid algorithm, oscillating coefficients, preconditioner
(20 pages, 2007)

112. L. Bonilla, T. Götz, A. Klar, N. Marheineke, R. Wegener
Hydrodynamic limit of the Fokker-Planck-equation describing fiber lay-down processes
Keywords: stochastic dierential equations, Fokker-Planck equation, asymptotic expansion, Ornstein-Uhlenbeck process
(17 pages, 2007)

113. S. Rief
Modeling and simulation of the pressing section of a paper machine
Keywords: paper machine, computational fluid dynamics, porous media
(41 pages, 2007)

114. R. Ciegis, O. Iliev, Z. Lakdawala
On parallel numerical algorithms for simulating industrial filtration problems
Keywords: Navier-Stokes-Brinkmann equations, finite volume discretization method, SIMPLE, parallel computing, data decomposition method
(24 pages, 2007)

115. N. Marheineke, R. Wegener
Dynamics of curved viscous fibers with surface tension
Keywords: Slender body theory, curved viscous bers with surface tension, free boundary value problem
(25 pages, 2007)

116. S. Feth, J. Franke, M. Speckert
Resampling-Methoden zur mse-Korrektur und Anwendungen in der Betriebsfestigkeit
Keywords: Weibull, Bootstrap, Maximum-Likelihood, Betriebsfestigkeit
(16 pages, 2007)

117. H. Knaf
Kernel Fisher discriminant functions – a concise and rigorous introduction
Keywords: wild bootstrap test, texture classification, textile quality control, defect detection, kernel estimate, nonparametric regression
(30 pages, 2007)

118. O. Iliev, I. Rybak
On numerical upscaling for flows in heterogeneous porous media
Keywords: numerical upscaling, heterogeneous porous media, single phase flow, Darcy's law, multiscale problem, effective permeability, multipoint flux approximation, anisotropy
(17 pages, 2007)

119. O. Iliev, I. Rybak
On approximation property of multipoint flux approximation method
Keywords: Multipoint flux approximation, finite volume method, elliptic equation, discontinuous tensor coefficients, anisotropy
(15 pages, 2007)

120. O. Iliev, I. Rybak, J. Willems
On upscaling heat conductivity for a class of industrial problems
Keywords: Multiscale problems, effective heat conductivity, numerical upscaling, domain decomposition
(21 pages, 2007)

121. R. Ewing, O. Iliev, R. Lazarov, I. Rybak
On two-level preconditioners for flow in porous media
Keywords: Multiscale problem, Darcy's law, single phase flow, anisotropic heterogeneous porous media, numerical upscaling, multigrid, domain decomposition, efficient preconditioner
(18 pages, 2007)

122. M. Brickenstein, A. Dreyer
POLYBORI: A Gröbner basis framework for Boolean polynomials
Keywords: Gröbner basis, formal verification, Boolean polynomials, algebraic cryptoanalysis, satisfiability
(23 pages, 2007)

123. O. Wirjadi
Survey of 3d image segmentation methods
Keywords: image processing, 3d, image segmentation, binarization
(20 pages, 2007)

124. S. Zeytun, A. Gupta
A Comparative Study of the Vasicek and the CIR Model of the Short Rate
Keywords: interest rates, Vasicek model, CIR-model, calibration, parameter estimation
(17 pages, 2007)

125. G. Hanselmann, A. Sarishvili
Heterogeneous redundancy in software quality prediction using a hybrid Bayesian approach
Keywords: reliability prediction, fault prediction, non-homogeneous poisson process, Bayesian model averaging
(17 pages, 2007)

126. V. Maag, M. Berger, A. Winterfeld, K.-H. Küfer
A novel non-linear approach to minimal area rectangular packing
Keywords: rectangular packing, non-overlapping constraints, non-linear optimization, regularization, relaxation
(18 pages, 2007)

127. M. Monz, K.-H. Küfer, T. Bortfeld, C. Thieke
Pareto navigation – systematic multi-criteria-based IMRT treatment plan determination
Keywords: convex, interactive multi-objective optimization, intensity modulated radiotherapy planning
(15 pages, 2007)

128. M. Krause, A. Scherrer
On the role of modeling parameters in IMRT plan optimization
Keywords: intensity-modulated radiotherapy (IMRT), inverse IMRT planning, convex optimization, sensitivity analysis, elasticity, modeling parameters, equivalent uniform dose (EUD)
(18 pages, 2007)

129. A. Wiegmann
Computation of the permeability of porous materials from their microstructure by FFF-Stokes
Keywords: permeability, numerical homogenization, fast Stokes solver
(24 pages, 2007)

Status quo: November 2007